Density-functional and hydrodynamical approach to ion-atom collisions through a new generalized nonlinear Schrödinger equation

B. M. Deb and P. K. Chattaraj
Theoretical Chemistry Group, Department of Chemistry, Panjab University, Chandigarh 160014, India
(Received 7 July 1987; revised manuscript received 19 July 1988)

This paper proposes a quantum-fluid density-functional theory (an interlinking of quantum-fluid dynamics and density-functional theory) for dealing with molecular collisions, in order to incorporate both time dependence and excited states. Using a new kinetic energy density functional for ion-atom collisions, we have derived a single-particle time-dependent single density equation for many-electron systems. The equation is a new generalized nonlinear Schrödinger equation whose solution directly yields the time-dependent charge density, current density, and a pulsating effective potential surface on which the process occurs. The new equation is also derived through Nelson's stochastic interpretation of the single-particle Schrödinger equation. A "thermodynamics" of the entire time-evolving system is suggested in terms of space- and time-dependent quantities. New algorithms have been devised for solving the above equation in one and two spatial dimensions, in a succession of time steps. Results have been obtained and analyzed in the approach regime for proton-neon high-energy (25-keV) collisions, which permit excitation but not ionization. These results show distinct nonlinear features.

I. INTRODUCTION

During the last two decades, density-based theories[1-17] of many-electron systems, in particular, density-functional theory (DFT), have been very successful in explaining the electronic structure, binding, and properties of atoms, molecules, and solids, including surfaces. However, these developments have largely been restricted to time-independent situations and to the ground state. For example, molecular reaction dynamics, involving atomic, molecular, and gas-surface[18] collisions, have remained outside DFT. It has been our view[12,15,19-22] that DFT and quantum-fluid dynamics (QFD), i.e., the hydrodynamical analogy to quantum mechanics, should jointly form a quamtum theory of many-electron systems in which the many-electron wave function is replaced by the single-particle charge density and current density. This method has the advantage of treating dynamical processes evolving in time in terms of a single, one-particle time-dependent (TD) equation which is essentially a generalization[23,24] of time-independent single-density equations derived by several workers.[25-29] Because of the hydrodynamical analogy, it has also a bearing on "classical" interpretations of quantum mechanics as well as on a "thermodynamic" description of an individual many-electron system.

Apart from the problems of time dependence and excited states, the absence of a satisfactory kinetic energy density (KED) functional with proper local and global behavior as well as a proper functional derivative poses difficulties. All these three problems are incorporated in this paper. In Sec. II A we describe the KED functional employed in the present work on proton-neon high-energy collisions. Section II B uses this functional along with QFD equations to derive the TD single-density equation (SDE) for the collisional process. The equation is a new generalized nonlinear Schrödinger equation (GNLSE).[23] Section II C derives the same TDSDE from a stochastic interpretation[30-37] of the single-particle Schrödinger equation. Section III deals with certain "thermodynamic" implications for the electron cloud whose motion is governed by the TDSDE. Section IV describes the finite-difference (FD) schemes employed for solving the TDSDE in one and two spatial dimensions. Results are discussed in terms of the TD charge density, current density, effective potential *(pulsating potential),* and chemical potential. Finally, Sec. V summarizes the new features presented in this work.

II. TIME-DEPENDENT SINGLE-PARTICLE DENSITY EQUATION FOR A MANY-ELECTRON SYSTEM

A. New KED functional for the proton-neon colliding system

Figure 1 depicts the colliding system (proton energy, 25 keV) in a rotating coordinate frame. In view of the high energy, a straight-line approximation[38-42] is adopted in order to fix the classical trajectory on which the two nuclei move. The trajectory $R(t)$ is given by

$$R(t)=[b^2+z^2(t)]^{1/2}\ , \tag{1a}$$

$$z(t)=[z(0)-v_p t]\ , \tag{1b}$$

where the "time" t is a positive semidefinite parameter; $z(t)$ is positive when the proton has not reached 0 and negative when it has crossed 0. However, when the projectile energy is of the order of, say, 50 eV, as happens in reactive collisions, the straight-line approximation is not valid. One may then solve classical equations of motion, incorporating the quantum-mechanical electron density, in order to obtain the nuclear trajectory.

The kinetic energy of the interacting system (a "supermolecule") consists of an atomic and a molecular part, viz.

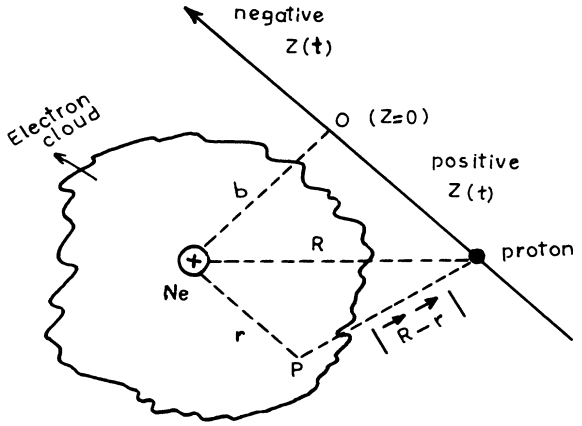

FIG. 1. Physical model of the proton-neon atom scattering system in a rotating coordinate frame. The proton moves in a straight line with velocity v_p and impact parameter b. The target Ne nucleus is placed at the origin and the $z(t)$ coordinate of the proton is measured relative to the point 0. b has been taken as either 1 a.u. (one-dimensional case) or 0 (two-dimensional case); $v_p=1$ a.u. (energy, 25 keV). R is the internuclear distance and r is the distance of a point P from the Ne nucleus.

$$T[\rho]=\int\{t_{\rm at}[\rho]+t_{\rm mol}[\rho]\}d\mathbf{r}\ , \tag{2}$$

where ρ is the electron density of the interacting system at the internuclear distance R. The atomic and molecular KED's are taken, respectively, as (N is the total number of electrons)

$$t_{\rm at}[\rho]=C_k\rho^{5/3}+\frac{1}{8}\frac{(\nabla\rho)^2}{\rho}+a(N)\left[\frac{\mathbf{r}\cdot\nabla\rho}{r^2}-\tfrac{1}{2}\nabla^2\rho\right]\ , \tag{3}$$

$$t_{\rm mol}[\rho]=\frac{f(R,N)}{N}\rho\ , \tag{4a}$$

$$f(R,N)=\frac{1}{R^{12}}-(N/10)^{14}R^2\exp(-0.8R)\ , \tag{4b}$$

where $C_k=(3/10)(3\pi^2)^{2/3}$ and $a(N)$ is taken from Ghosh and Balbas.[43] In Eq. (3) the first term in square brackets is the "first gradient" correction discussed by us before;[44,45] in particular, it leads to excellent atomic kinetic energy, both locally and globally. In (4b), $f(R,N)$ satisfies the following properties: (i) $t_{\rm mol}[\rho]\to 0$ when $R\to\infty$; (ii) diatomic molecular kinetic energies at $R_{\rm eq}$, calculated by using Eqs. (2)–(4) and double-ζ molecular densities,[46] are in fairly good agreement (Table I) with the corresponding double-ζ values (except for H_2 for which the Weizsäcker term itself gives a good estimate of the kinetic energy); (iii) a comparison between the behavior of

$$\Delta T(R)=T(R)-T(\infty)=\int t_{\rm mol}d\mathbf{r}=f(R,N)\ , \tag{5}$$

with respect to R, for a diatomic molecule with $N=10$ (Fig. 2), and that for the H_2 molecule[47,48] shows that (a) the qualitative nature of the ΔT curve is the same in both cases, (b) $\lim_{R\to 0,\infty}\Delta T(R)$ exhibits the same behavior, and (c) the position of the minimum in ΔT (Fig. 2) is physically reasonable. Thus, there are excellent reasons for employing Eqs. (2)–(4).

TABLE I. Molecular kinetic energies calculated according to Eq. (2) using double-ζ wave functions (Ref. 46). All values are in atomic units.

Molecule	Kinetic energy Eq. (2)	Kinetic energy Double-ζ[a]
H_2	1.4791	1.128
HF	99.8495	100.01
N_2	94.2594	108.74
BF	130.3136	124.17
CO	111.2529	112.65

[a]Reference 46.

B. Time-dependent generalized nonlinear Schrödinger equation in three-dimensional space

In this section we derive an SDE for calculating the TD charge density and current density so that one can, in principle, follow the collisional process from "start" to "finish." In view of the current status of TDDFT,[37] we assume the validity of the QFD equations, involving familiar DFT quantities, in three-dimensional (3D) space, viz. a continuity equation and an equation of motion:[17,21]

$$\frac{\partial\rho}{\partial t}+\nabla\cdot(\rho\nabla\chi)=0\ , \tag{6}$$

$$\frac{\partial\chi}{\partial t}+\tfrac{1}{2}(\nabla\chi)^2+\frac{\delta G[\rho]}{\delta\rho}+\int\frac{\rho(\mathbf{r}',t)}{|\mathbf{r}-\mathbf{r}'|}d\mathbf{r}'+v(\mathbf{r},t)=0\ , \tag{7}$$

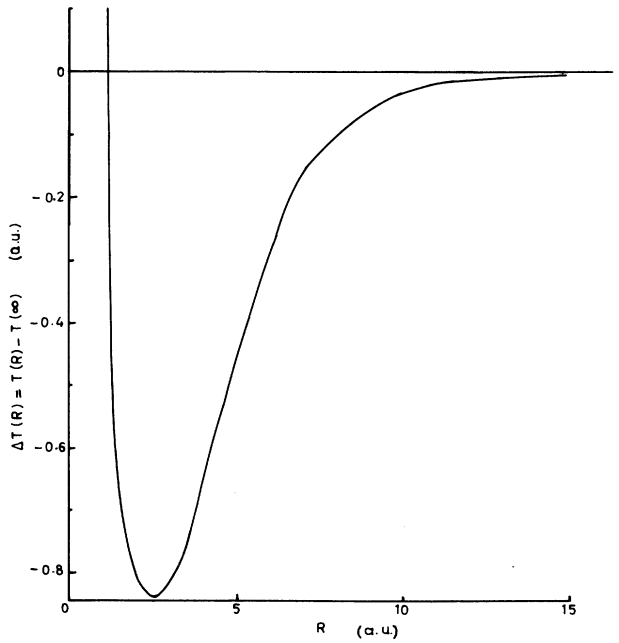

FIG. 2. Change in electronic kinetic energy on molecule formation, according to Eq. (5), as a function of the internuclear distance for a diatomic molecule containing ten electrons.

where $G[\rho]$ consists of kinetic[49] and exchange-correlation (XC) contributions, $v(\mathbf{r},t)$ is an external potential in one-to-one correspondence with the density $\rho(\mathbf{r},t)$ for all t; $\rho(\mathbf{r},t)$ is written in terms of a complex-valued function $\phi(\mathbf{r},t)$ and a real-valued velocity potential $\chi(\mathbf{r},t)$ as

$$\phi=\rho^{1/2}\exp(i\chi) , \tag{8a}$$

i.e.,

$$\rho=\phi^2\exp(-2i\chi)=|\phi|^2 . \tag{8b}$$

The initial density vanishes at infinity, the time-dependent potential is bounded, and its derivatives are well-behaved:[50-52]

$$G[\rho]=T[\rho]+E_{\rm XC}[\rho] , \tag{9}$$

$$E_{\rm XC}[\rho]=E_x[\rho]+E_c[\rho] , \tag{10}$$

$$E_x[\rho]=-C_x\int\rho^{4/3}d\mathbf{r},\quad C_x=(\tfrac{3}{4}\pi)(3\pi^2)^{1/3} . \tag{11}$$

In the present work, $E_c[\rho]$ is neglected in order to reduce nonlinearity in the final SDE although a local correlation functional can be incorporated, in principle. Also, for proton-atom collisions,

$$v(\mathbf{r},t)=v(\mathbf{r},\mathbf{R},t)=-\left[\frac{Z}{r}+\frac{1}{|\mathbf{R}(t)-\mathbf{r}|}\right] , \tag{12}$$

where Z is the nuclear charge of the atom and $\mathbf{R}(t)$ is the Coulomb trajectory on which the two nuclei move (Fig. 1). In general, $v(\mathbf{r},t)$ may also contain an external TD perturbation.

As shown in the Appendix, if one uses Eqs. (8) and eliminates χ between Eqs. (6) and (7), there results the following new GNLSE of a type and complexity never encountered:

$$[-\tfrac{1}{2}\nabla^2+v_{\rm eff}(\mathbf{r},t)]\phi(\mathbf{r},t)=i\frac{\partial\phi(\mathbf{r},t)}{\partial t} , \tag{13}$$

where $v_{\rm eff}(\mathbf{r},t)\equiv v_{\rm eff}(\mathbf{r},\mathbf{R},t)$ is a pulsating potential surface governing the TD process under consideration and is written as

$$v_{\rm eff}=\tfrac{5}{3}C_k\rho^{2/3}-\tfrac{4}{3}C_x\rho^{1/3}-\frac{a(N)}{r^2}-\frac{Q(\mathbf{r})}{r}-\frac{1}{|\mathbf{R}-\mathbf{r}|}+\frac{f(R,N)}{N} , \tag{14}$$

with the screened nuclear charge $Q(\mathbf{r})$ given by

$$Q(\mathbf{r})=Z-r\int\frac{\rho(\mathbf{r}',t)}{|\mathbf{r}-\mathbf{r}'|}d\mathbf{r}' . \tag{15}$$

In molecular collision theory, Macias and Riera[53] have discussed the use of reaction coordinates which depend both on nuclear and electronic coordinates.

Equations (13)–(15) form the backbone of the present QFDFT (quantum-fluid density-functional theory) approach. It is obvious that while Eq. (13) maintains time-reversal symmetry, its solution ϕ does not obey the superposition principle. Equation (13) may be formally regarded as describing the dynamics of a "noninteracting" system of particles where the kinetic energy part is represented by the Laplacian operator and all relevant interactions are incorporated in $v_{\rm eff}$. Note, however, that the Laplacian in Eq. (13) does not arise from a "noninteracting" kinetic energy but from the Weizsäcker term in Eq. (3). Nevertheless, the above interpretation is consistent since the partitioning in Eq. (9) neglects the coupling between kinetic energy and electronic interaction.

The nonlinearity in Eq. (13) arises from both nonintegral powers of ϕ (or ρ) and the integral in $Q(\mathbf{r})$. As shown in Sec. IV, the numerical solution of Eq. (13) yields $v_{\rm eff}(\mathbf{r},t)$ and the TD single "orbital" $\phi(\mathbf{r},t)$ for the many-electron system, whose modulus square yields the charge density $\rho(\mathbf{r},t)$ and whose phase leads to the current density $\mathbf{j}(\mathbf{r},t)$. Investigations into the mathematical significance of Eq. (13) may have an important bearing on the theory of nonlinear equations; especially, studies on the integrability properties of such an equation may indicate the possibility or otherwise of quantum chaos in certain TD phenomena. It is also conceivable that when the time-evolving dispersive and nonlinear terms balance each other, solitons or solitary waves may be generated. In other words, Eq. (13) provides a new way of extracting information about dynamical processes through $\rho(\mathbf{r},t)$, $\mathbf{j}(\mathbf{r},t)$, and $v_{\rm eff}(\mathbf{r},t)$, or any suitable partitioning of these quantities. Thus, $\rho(\mathbf{r},t)$ describes the dynamics of charge reorganization in the system due to the perturbation, in particular, the flow of charge from one region to another (local accumulation or depletion), collective density oscillations, etc. Initially ($t=0$), if the system is in the ground state, the current density $\mathbf{j}(\mathbf{r},t)$ vanishes. However, as the interaction progresses with time, $\mathbf{j}(\mathbf{r},t)$ will generally be nonvanishing since, under the influence of the perturbation, excited states can mix with the ground state. Since $\mathbf{j}=\rho\nabla\chi$, it can also convey information about streamlines, vorticities ("quantum whirlpools"), magnetic effects,[12,15] etc., generated by the perturbation. Earlier proposals[25-29,45] for directly calculating ρ through a single equation corresponded to only static (time-independent) cases and in only two instances[26,45] were such equations actually solved. However, the phase part of the "orbital" function ϕ was not calculated before; the present work reports the first DFT calculation of both the amplitude and phase of ϕ. Note that, for a general excited state, the phase function (or the velocity potential) χ is not constant in space. Thus, any attempt to deal with excited states in a DFT framework should include both $\rho^{1/2}$ and χ. Although there have been extensions of the Hohenberg-Kohn theorem to excited states, such extensions are valid only for static (zero current-density) stationary states[15] and ensembles of states. Kohn and Vashishta[54(a)] concluded that self-consistent Kohn-Sham (KS) equations generally do not exist for excited states. However, such equations exist for ensembles of states.[54(b)-54(d)] In the present work $v_{\rm eff}(\mathbf{r},t)\to 0$ as $r\to\infty$, for all t, like the static KS potential and the $v_{\rm eff}(\mathbf{r})$ defined by Deb and Ghosh[26] and Levy *et al.*[28] This means that in the present ion-atom collision process, excitation is permitted but ionization is not. The approach here also satisfies the conditions of theorems 2 and 3 of Runge and Gross,[50] required for the calculation

of ρ and $\mathbf{j}$ from QFD equations and an action principle, respectively. However, their theorem 4 describes $\rho(\mathbf{r},t)$ as a sum over occupied orbitals each of which satisfies a TDKS equation in which $v_{\text{eff}}(\mathbf{r},t)$ consists of a TD external potential $v(\mathbf{r},t)$, Coulomb, and *XC* terms (this was an extension of the earlier TDKS equation of Deb and Ghosh[17]). The present TDSDE appears preferable to the usual TDKS, TDHF (Hartree-Fock),[38,55] and TDTF (Thomas-Fermi) (Refs. 39–42) approaches, all of which require the solution of more than one equation for many-electron systems.[56]

C. Derivation of Eq. (13) from forward and backward Fokker-Planck equations

Following Nelson's stochastic mechanics, we will now show the correspondence between the single-particle QFDFT Eq. (13) dealing with the motion of a generalized Madelung fluid and the classical dynamics of a particle of mass m undergoing diffusion in a medium with diffusion coefficient ν according to a Markov process.

Let the state of the system at a time t be characterized by a random position variable $\mathbf{r}(t)$ given by the Langevin equation

$$d\mathbf{r}(t)=\mathbf{b}(\mathbf{r},t)dt+d\mathbf{w}(r,t)\ , \tag{16}$$

where $\mathbf{b}$ is a forward diffusion function (drift) of space time and $d\mathbf{w}$ is a random variable normally distributed with mean zero and variance $\sigma^2(\mathbf{r},t)dt$. The probability density $\rho(\mathbf{r},t)$ satisfies both forward and backward Fokker-Planck equations

$$\frac{\partial\rho}{\partial t}=-\nabla\cdot(\mathbf{b}\rho)+\nu\nabla^2\rho\ , \tag{17a}$$

$$\frac{\partial\rho}{\partial t}=-\nabla\cdot(\mathbf{b}_*\rho)-\nu\nabla^2\rho\ , \tag{17b}$$

where $\mathbf{b}_*$ corresponds to backward diffusion in time. Taking the current velocity $\mathbf{v}(\mathbf{r},t)$ and the stochastic (osmotic) velocity $\mathbf{u}(\mathbf{r},t)$ as

$$\mathbf{v}=\tfrac{1}{2}(\mathbf{b}+\mathbf{b}_*)\ , \tag{18}$$

$$\mathbf{u}=\tfrac{1}{2}(\mathbf{b}-\mathbf{b}_*)\ , \tag{19}$$

and using Nelson's definitions[30] of the mean derivative and the mean acceleration $(\mathbf{F}/m)$, one can show that Eqs. (17a) and (17b) lead to two fluid dynamical equations

$$\frac{\partial\rho}{\partial t}=-\nabla\cdot(\rho\mathbf{v})\ , \tag{20}$$

$$\frac{\partial\mathbf{v}}{\partial t}=\frac{\mathbf{F}}{m}+(\mathbf{u}\cdot\nabla)\mathbf{u}-(\mathbf{v}\cdot\nabla)\mathbf{v}+\frac{\sigma^2}{2}\nabla(\nabla\cdot\mathbf{u})\ , \tag{21}$$

where $\mathbf{F}$ is the Newtonian force acting on the particle. The diffusion process being considered here differs from classical diffusion processes in two respects (i) It is nonlinear. (ii) The drift $\mathbf{b}(\mathbf{r},t)$ is not a preassigned vector field, but depends on the solution of Eqs. (20) and (21) at some initial time t_0.

It is worthwhile to note the striking formal similarity between Eqs. (20), (21) and the QFD Eqs. (6), (7). If one takes the mass of the diffusing quasiparticle as that of an electron, moving under a Newtonian force arising from an effective potential $v_{\text{eff}}(\mathbf{r},t)$, then one can obtain Eq. (13), as shown below. In other words, the two viewpoints, QFDFT and stochastic (Markovian), become equivalent making it possible to pass from one viewpoint to the other.[57–59]

In order to obtain Eq. (13), define a complex-valued function $\phi(\mathbf{r},t)$ as

$$\phi(\mathbf{r},t)=\rho^{1/2}(\mathbf{r},t)\exp[i\chi(\mathbf{r}t)]\ , \tag{8a'}$$

where

$$v=\sigma^2\nabla\chi\ . \tag{22}$$

We also have

$$\mathbf{u}=\frac{\sigma^2}{2}\frac{\nabla\rho}{\rho}\ , \tag{23}$$

$$\mathbf{F}=-\nabla v_{\text{eff}}\ . \tag{24}$$

Using Eqs. (8a') and (22)–(24) and eliminating χ (as in Sec. II B) between Eqs. (20) and (21) lead to an equation governing the dynamics of the given Brownian quasiparticle of mass m,

$$\left[-\frac{\sigma^2}{2}\nabla^2+\frac{1}{m\sigma^2}v_{\text{eff}}\right]\phi=i\frac{\partial\phi}{\partial t}\ . \tag{25}$$

Taking $\sigma^2=2\nu=\hbar/m$, Eq. (25) becomes (in a.u.)

$$[-\tfrac{1}{2}\nabla^2+v_{\text{eff}}]\phi=i\frac{\partial\phi}{\partial t}\ . \tag{13'}$$

This makes the interconnections between stochastic mechanics, fluid dynamics, and quantum mechanics transparent and interesting.

III. TOWARDS A "THERMODYNAMICS" OF AN INDIVIDUAL MOLECULAR SYSTEM

As an extension of the time-independent work of Ghosh *et al.*[60,61] for ground-state DFT, one may look at the dynamics of the problem in terms of a *space-time-dependent* "temperature," entropy density, and chemical potential for the entire time-evolving system. In particular, it may be worthwhile to study the changes in the chemical potential $\mu(\mathbf{r},t)$ which is related to both $v_{\text{eff}}(\mathbf{r},t)$ and $\rho(\mathbf{r},t)$. Thus, v_{eff} acts as a bridge between molecular reaction dynamics and molecular "thermodynamics." For this purpose, one recalls that through Eq. (13) one may consider the N-electron system as an *ideal* system of N noninteracting particles moving under the potential $v_{\text{eff}}(\mathbf{r},t)$ and, by analogy, bring in the required classical relations for an ideal monatomic gas by replacing the average number density N/V locally by $\rho(\mathbf{r},t)$. Thus, one may use the following "thermodynamic" relations (Θ is the temperature while k is the Boltzmann constant; atomic units are not employed in this section):

$$t_s(\mathbf{r};\rho(\mathbf{r},t))=\tfrac{3}{2}\rho(\mathbf{r},t)k\Theta(\mathbf{r},t)\ , \tag{26}$$

$$PV=Nk\Theta\ , \tag{27}$$

$$U=\tfrac{3}{2}Nk\Theta\ , \tag{28}$$

$$dS=\frac{1}{\Theta}(dU+PdV)\ , \tag{29}$$

$$E=U+V_{\text{eff}}\ , \tag{30}$$

$$\left[\frac{\partial V_{\text{eff}}}{\partial N}\right]_{\Theta,P}=v_{\text{eff}}(\mathbf{r},t)\ , \tag{31}$$

$$\Theta dS=dE+PdV-\mu dN\ , \tag{32}$$

$$S=\tfrac{3}{2}Nk+Nk\ln\left[\left[\frac{2\pi mk\Theta}{h^2}\right]^{3/2}\frac{V}{N}e\right]\ , \tag{33}$$

$$G=\tfrac{5}{2}Nk\Theta+V_{\text{eff}}-\Theta S\ , \tag{34}$$

$$\mu=\left[\frac{\partial G}{\partial N}\right]_{\Theta,P}\ . \tag{35}$$

Below, we will obtain a more general expression than Eq. (26). For the present, replacing N/V by $\rho(\mathbf{r},t)$, Eqs. (26)–(35) lead to the following expressions for the entropy density $s(\mathbf{r},t)$ and the chemical potential $\mu(\mathbf{r},t)$ through alternative routes:

$$\frac{S}{V}\equiv s(\mathbf{r},t)=\tfrac{3}{2}k\rho\ln\Theta-k\rho\ln\rho+\tfrac{1}{2}k\rho\left[5+3\ln\left[\frac{2\pi mk}{h^2}\right]\right]\ , \tag{36}$$

$$\mu(\mathbf{r},t)=v_{\text{eff}}+k\Theta\ln\rho-\tfrac{3}{2}k\Theta\ln\left[\frac{2\pi mk\Theta}{h^2}\right]\ . \tag{37}$$

Equations (36) and (37) may also be obtained from information theory by constructing a generalized Shanon entropy in terms of $\rho(\mathbf{r},t)$ and then maximizing the entropy subject to appropriate constraints. Note that no thermal property is being ascribed to the temperature Θ.

Since the time evolution of the system is envisaged in terms of the "classical" flow of a quantum fluid, the flow of $\mu(\mathbf{r},t)$ may be utilized to define microscopic rate constants (c.f., Parr's[62] definition of a distorted chemical potential in a static framework). According to ground-state DFT, the chemical potential of the entire system is constant all over space at both the beginning and the end of the process; therefore, $\mu(\mathbf{r},t)$ describes the dynamical evolution of the system from μ_{initial} to μ_{final}.

We now push the thermodynamic analogy further by bringing in a local entropy current density $\mathbf{j}_s(\mathbf{r},t)$ and a local entropy production $\bar{\sigma}(\mathbf{r},t)$ such that the following relation[63] holds:

$$\frac{\partial s(\mathbf{r},t)}{\partial t}+\nabla\cdot\mathbf{j}_s(\mathbf{r},t)=\bar{\sigma}(\mathbf{r},t)\ , \tag{38}$$

where $s(\mathbf{r},t)$ is given by Eq. (36). Below, we obtain an expression for $\bar{\sigma}(\mathbf{r},t)$.

Define a velocity field $\mathbf{v}_s$ for entropy flow as

$$\mathbf{j}_s(\mathbf{r},t)=s(\mathbf{r},t)\mathbf{v}_s(\mathbf{r},t) \tag{39}$$

and recall that the current density $\mathbf{j}(\mathbf{r},t)$ is defined as

$$\mathbf{j}(\mathbf{r},t)=\rho(\mathbf{r},t)\mathbf{v}(\mathbf{r},t)\ . \tag{40}$$

We will use the ansatz

$$\mathbf{v}_s(\mathbf{r},t)=\mathbf{v}(\mathbf{r},t) \tag{41}$$

and employ a phase-space Maxwellian distribution function $f(\mathbf{r},\mathbf{p},t)$ of the form

$$f(\mathbf{r},\mathbf{p},t)=L(\mathbf{r},t)\exp[-p^2/2mk\Theta(\mathbf{r},t)]\ , \tag{42}$$

where

$$L(\mathbf{r},t)=\left[\frac{h^2}{2\pi mk\Theta(\mathbf{r},t)}\right]^{3/2}\rho(\mathbf{r},t)\ . \tag{43}$$

This form for $L(\mathbf{r},t)$ may be obtained in two ways: (i) by taking $f(\mathbf{r},\mathbf{p},t)$ as

$$f(\mathbf{r},\mathbf{p},t)=\exp[\mu(\mathbf{r},t)/k\Theta(\mathbf{r},t)]\times\exp\{-[p^2/2m+v_{\text{eff}}(\mathbf{r},t)]/k\Theta(\mathbf{r},t)\} \tag{44}$$

and using Eq. (37) for $\mu(\mathbf{r},t)$, and (ii) by taking $f(\mathbf{r},\mathbf{p},t)$ as

$$f(\mathbf{r},\mathbf{p},t)=\frac{N\exp[-p^2/2mk\Theta(\mathbf{r},t)]}{\frac{1}{h^3}\int\int\exp[-p^2/2mk\Theta(\mathbf{r},t)]d\mathbf{r}\,d\mathbf{p}}\ , \tag{45}$$

then replacing N/V locally by $\rho(\mathbf{r},t)$ and Θ by $\Theta(\mathbf{r},t)$. Here h^3 is the phase-space volume element and N occurs due to the normalization constraint

$$\frac{1}{h^3}\int\int f(\mathbf{r},\mathbf{p},t)d\mathbf{r}\,d\mathbf{p}=\int\rho(\mathbf{r},t)d\mathbf{r}=N\ . \tag{46}$$

If one defines the current density as

$$\mathbf{j}(\mathbf{r},t)=\frac{1}{h^3}\int\frac{\mathbf{p}}{m}f(\mathbf{r},\mathbf{p},t)d\mathbf{p}\ , \tag{47}$$

then $\mathbf{j}(\mathbf{r},t)$ vanishes for $f(\mathbf{r},\mathbf{p},t)$ defined as above. Therefore, this distribution $f(\mathbf{r},\mathbf{p},t)$ corresponds only to states with zero current density, e.g., the ground state. For a dynamical state, with nonzero current density, it is necessary to define $f(\mathbf{r},\mathbf{p},t)$ as

$$f(\mathbf{r},\mathbf{p},t)=L(\mathbf{r},t)\exp[-\alpha(t)(\mathbf{p}+\mathbf{p}_0)^2/2mk\Theta(\mathbf{r},t)]\ , \tag{48}$$

where $\alpha(t)$ is a TD scalar variable and $\mathbf{p}_0$ is a constant additive factor having the dimension of momentum. $\mathbf{p}_0$ vanishes for states with zero current density while $\alpha(t)$ turns out to be unity if normalization is preserved [this may be seen by putting (48) into (46)]. Thus,

$$f(\mathbf{r},\mathbf{p},t)=L(\mathbf{r},t)\exp[-(\mathbf{p}+\mathbf{p}_0)^2/2mk\Theta(\mathbf{r},t)]\ . \tag{49}$$

Since $f\to 0$ as $|\mathbf{p}|\to\infty$, $\Theta(\mathbf{r},t)>0$ $\forall\mathbf{r},t$. Substituting (49) into (47), we find

$$\mathbf{j}(\mathbf{r},t)=-\frac{\mathbf{p}_0}{m}\rho(\mathbf{r},t)\ . \tag{50}$$

The KED $t_s(\mathbf{r},\rho)$ may be obtained as

$$t_s(\mathbf{r},\rho)=\frac{1}{h^3}\int \frac{p^2}{2m}f(\mathbf{r},\mathbf{p},t)d\mathbf{p}$$
$$=\tfrac{3}{2}\rho(\mathbf{r},t)k\Theta(\mathbf{r},t)+\frac{p_0^2}{2m}\rho(\mathbf{r},t)$$
$$=\tfrac{3}{2}\rho k\Theta+\frac{|\mathbf{j}|^2 m}{2\rho}\ , \tag{51}$$

which is more general than Eq. (26). Using Eqs. (40) and (50), the velocity vector $\mathbf{v}$ turns out to be

$$\mathbf{v}=-\frac{\mathbf{p}_0}{m}\ . \tag{52}$$

Using the continuity equation

$$\frac{\partial\rho}{\partial t}+\nabla\cdot\mathbf{j}=0\ , \tag{53}$$

and taking $s(\mathbf{r},t)$ from Eq. (36), one obtains

$$\frac{\partial s}{\partial t}=k\rho\nabla\cdot\mathbf{v}-s\nabla\cdot\mathbf{v}-\mathbf{v}\cdot\nabla s+\tfrac{3}{2}\frac{k\rho}{\Theta}\mathbf{v}\cdot\nabla\Theta+\tfrac{3}{2}\frac{k\rho}{\Theta}\frac{\partial\Theta}{\partial t}\ . \tag{54}$$

Using (39) and the ansatz (41), Eq. (54) becomes

$$\frac{\partial s}{\partial t}=-\nabla\cdot\mathbf{j}_s+k\rho\nabla\cdot\mathbf{v}_s+\frac{3}{2}\frac{k\rho}{\Theta}\mathbf{v}_s\cdot\nabla\Theta+\frac{3}{2}\frac{k\rho}{\Theta}\frac{\partial\Theta}{\partial t}\ . \tag{55}$$

Since $\mathbf{p}_0$ is a constant additive factor,

$$\rho\nabla\cdot\mathbf{v}_s=-\frac{\rho}{m}\nabla\cdot\mathbf{p}_0=0\ . \tag{56}$$

Hence, Eq. (55) takes the form

$$\frac{\partial s}{\partial t}+\nabla\cdot\mathbf{j}_s=\tilde{\sigma}\ , \tag{38'}$$

where the entropy production $\tilde{\sigma}$ is given by

$$\tilde{\sigma}=\frac{3}{2}\frac{k\rho}{\Theta}\left[\mathbf{v}_s\cdot\nabla\Theta+\frac{\partial\Theta}{\partial t}\right]\ . \tag{57}$$

For a "static" stationary state

$$\frac{\partial\Theta}{\partial t}=0 \tag{58}$$

and then $\tilde{\sigma}$ becomes

$$\tilde{\sigma}=\frac{3}{2}\frac{k}{\Theta}(\mathbf{j}_s\cdot\nabla\Theta)\ . \tag{59}$$

Thus, it is worthwhile to note that although no thermal property is being ascribed to the quantity $\Theta(\mathbf{r},t)$, it is possible to write down an internally consistent set of "thermodynamic" relations involving ρ, $\mathbf{j}$, v_{eff}, μ, and Θ. Interestingly, the last term in Eq. (51) also occurs in the TD transient KED functional derived by Kohl and Dreizler[64] [see their Eq. (9)].

IV. NUMERICAL SOLUTION OF THE TDSDE (13)

A. Solution in one spatial dimension

There does not appear to be any general numerical or analytical method for solving GNLSE's and therefore each such equation has to be treated individually. For convenience, we approach the solution of Eq. (13) in two steps. The first step assumes Eq. (13) to have only one spatial dimension (apart from time), i.e., the colliding system is assumed (unrealistically) to have spherical symmetry. The second step considers the actual cylindrical symmetry of the system by taking two spatial dimensions; the third spatial variable, an azimuthal angle, is averaged out. The methods of solution adopted in the two cases are different, the second method being more general.

Taking the origin of electronic coordinates at the Ne nucleus and using the transformations

$$y(\mathbf{r},t)=r\phi(\mathbf{r},t)\ , \tag{60}$$

$$r=x^2\ , \tag{61}$$

Eq. (13) takes the form

$$\left[-\frac{1}{8x^2}\frac{\partial^2}{\partial x^2}+\frac{1}{8x^3}\frac{\partial}{\partial x}+v_{\text{eff}}\right]y=i\frac{\partial y}{\partial t}\ . \tag{62}$$

We have solved Eq. (62) by a Crank-Nicolson-type explicit-implicit finite-difference scheme.[65–69] The final set of difference equations, for any mesh point in t, is

$$c_j y_{j-1}+a_j y_j+b_j y_{j+1}=d_j\ , \tag{63}$$
$$j=1,2\ldots,M\ ,$$
$$c_1=b_M=0\ ,$$

(M is the number of mesh points in x) where

$$c_j=-i\left[\frac{1}{16x_j^3\Delta x}+\frac{1}{8x_j^2(\Delta x)^2}\right]\ , \tag{64}$$

$$a_j=\frac{2}{\Delta t}+iv_{\text{eff}}+\frac{1}{4x_j^2(\Delta x)^2}\ , \tag{65}$$

$$b_j=i\left[\frac{1}{16x_j^3\Delta x}-\frac{1}{8x_j^2(\Delta x)^2}\right]\ , \tag{66}$$

$$d_j=-\frac{i}{8x_j^3}\left[\frac{y_{m+1}^n-y_{m-1}^n}{2\Delta x}\right]+\frac{i}{8x_j^2}\left[\frac{y_{m+1}^n-2y_m^n+y_{m-1}^n}{(\Delta x)^2}\right]+\left[\frac{2}{\Delta t}-iv_{\text{eff}}\right]y_m^n\ . \tag{67}$$

In Eqs. (64)–(67), Δx and Δt are the step sizes while m and n are the mesh points in x and t, respectively. The mesh sizes adopted are $\Delta x=0.01$ a.u. and $\Delta t=0.01$ a.u. In Eq. (67), the first two terms set within large parentheses denote the explicit finite difference approximations of $(\partial y/\partial x)$ and $(\partial^2 y/\partial x^2)$, respectively.

The resulting matrix equation is tridiagonal and has

been solved by using a modified Thomas algorithm. The matrix equation is

$$\begin{bmatrix} a_1 & b_1 & & & \\ c_2 & a_2 & b_2 & & [0] \\ & \ddots & \ddots & \ddots & \\ [0] & & \ddots & \ddots & b_{M-1} \\ & & & c_M & a_M \end{bmatrix} \begin{bmatrix} y_1 \\ y_2 \\ \vdots \\ \vdots \\ y_M \end{bmatrix} = \begin{bmatrix} d_1 \\ d_2 \\ \vdots \\ \vdots \\ d_M \end{bmatrix} , \tag{68}$$

$$y \to 0 \quad \text{as } r \to 0, \infty \quad \forall t . \tag{69}$$

The modified Thomas algorithm consists of the following three steps:

(i) Compute β_j as follows:

$$\beta_1 = a_1 ,$$

$$\beta_j = a_j - \frac{c_j b_{j-1}}{\beta_{j-1}}, \quad j = 2, \ldots, M . \tag{70}$$

(ii) Compute γ_j as follows:

$$\gamma_1 = d_1 ,$$

$$\gamma_j = d_j - \frac{c_j \gamma_{j-1}}{\beta_{j-1}}, \quad j = 2, \ldots, M . \tag{71}$$

(iii) Compute y_j as follows:

$$y_M = \frac{\gamma_M}{\beta_M} ,$$

$$y_j = \frac{\gamma_j - b_j y_{j+1}}{\beta_j}, \quad j = M-1, \ldots, 3, 2, 1 . \tag{72}$$

The process of solution is launched with a trial value of y_m^n (in the present case, this is taken from a near-Hartree-Fock wave function[70] for Ne) in order to first obtain v_{eff} and then d_j. Next, the tridiagonal matrix equation (68) is solved self-consistently subject to the boundary conditions (69) in order to obtain y_m^{n+1} for all m. The existence of a variational minimum for all t is tacitly assumed. At a particular t, we first obtain the $(y_m^{n+1})^{\text{old}}$ from the previous t; the matrix equation is solved by using this $(y_m^{n+1})^{\text{old}}$. If this solution, $(\bar{y}_m^{n+1})$, is far removed from $(y_m^{n+1})^{\text{old}}$. If this solution, $(\bar{y}_m^{n+1})$, is far removed from $(y_m^{n+1})^{\text{old}}$ then we take a suitable mixture of the two as

$$(y_m^{n+1})^{\text{new}} = \alpha \bar{y}_m^{n+1} + (y_m^{n+1})^{\text{old}}(1-\alpha) , \tag{73}$$

where the fraction α is a mixing coefficient (0.5 in the present case). At this point we apply the following self-consistent criterion:

$$\frac{|(y_m^{n+1})^{\text{old}} - \bar{y}_m^{n+1}|}{\bar{y}_m^{n+1}} \leq \delta \quad \forall m , \tag{74}$$

where δ is a preassigned small positive number (0.01 in the present case).

The inner iteration is continued until condition (74) is satisfied. In the inner iteration, $(y_m^{n+1})^{\text{new}}$ is taken as $(y_m^{n+1})^{\text{old}}$ and the entire process is repeated. Throughout the inner iteration, v_{eff} in d_j is kept fixed whereas v_{eff} in a_j is recalculated using the new $(y_m^{n+1})^{\text{new}}$. For a particular t, when the self-consistent solution from the inner iteration $(\bar{y}_m^{n+1})$ is obtained, we increase the time by Δt in order to go to the next point of time. After calculating v_{eff} and then d_j, using $\bar{y}_m^{n+1}$, the whole process of inner iteration is again repeated until self-consistency is reached. For four time steps, we have also checked the calculations with $\delta = 0.001$; this increases the number of iterations required, with very little change in the final self-consistent solution. In every iteration, normalization (i.e., the total number of electrons) is conserved within the computation grid. This permits excitation but not ionization. The whole scheme is rapidly convergent.

The Crank-Nicolson scheme applied here is unconditionally stable and consistent with the original parabolic partial differential equation (62). As a preliminary physical test, using the same algorithm, we have solved the well-known cubic nonlinear Schrödinger equation[71,72] where a sech-type soliton pulse is moved forward by 41 time steps and then taken back to its initial position where the original profile is reproduced within the prescribed tolerance limit. In this backward evolution in time, there is no cancellation of errors with those from the forward evolution.

We have performed rigorous stability, consistency and convergence tests for the finite difference scheme adopted here. The stability analysis was performed[73] using both Von Neumann's Fourier series method and the matrix method. It was found that for quantum-mechanical equations of motion, stability of FD schemes depend on both spatial and temporal zoning and thus the usual Fourier series method is inadequate whereas the matrix method is satisfactory. The consistency analysis was performed through the Taylor expansion of the variable concerned at different mesh points and the calculation of truncation error. The truncation error is of second order in both Δx and Δt, going to zero as Δx and Δt go to zero. Thus, the FD analogue (63) is consistent with Eq. (62), stable, and convergent.

We have solved the spherically symmetric case for 61 time steps to calculate $\rho(\mathbf{r},t)$, the radial density $4\pi r^2 \rho(\mathbf{r},t)$, and $v_{\text{eff}}(\mathbf{r},t)$. The current density and chemical potential have been calculated only for the cylindrically symmetric case.

B. Interpretation of one-dimensional results

One may visualize the entire collisional process as consisting of *approach, encounter,* and *departure* regimes. Since $R = 10.05$ a.u. at $t = 0$ and $\Delta t = 0.01$ a.u., in these calculations the proton is essentially in the approach regime. Figures 3 and 4 depict the TD radial density and v_{eff} at selected intervals of time.

1. TD radial density

Figure 3 shows that the initial two peaks in the radial density of Ne, characteristic of its shell structure, tend to give way to only one peak. This occurs because the initial input of near-Hartree-Fock density is not a solution of the TD density equation (13) and is transformed over

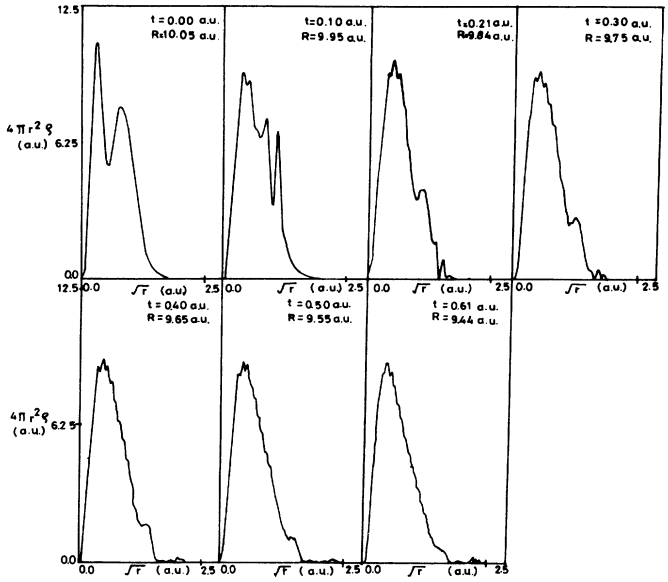

FIG. 3. Multiwindow plot of radial density against $\sqrt{r}$ for the proton-neon scattering system ($v_p = 1$, $b = 1$ a.u.) up to 61 time steps, in the spherically symmetric approximation.

the course of time into a shell-structureless, almost stable, TFD-like profile. The change occurs by a reduction in height plus shifting to right of the first peak and gradual subsiding of the second peak. Interestingly, a crownlike structure of the surviving peak persists, seemingly as a reminder of the shell structure. The crown separates the inner part ("core region") from the outer part ("valence region") which becomes progressively more diffuse due to the attraction by the incoming proton. The smooth inner part (to the left of the crown) hardly undergoes any significant change from 21 to 61 time steps. Even the peak height remains almost the same after 30 time steps. Thus, a distinct *nonlinear* feature is revealed in these radial density plots, with the inner part remaining smooth and practically unchanged (at least between 30 and 61 time steps) while the outer part becomes more diffuse and develops structures. In other words, as the projectile approaches, the inner part of the Ne density does not oscillate while the outer part does. Earlier plots of time-evolving electronic probability density for α-H collisions at high energies had revealed "significant unphysical noise."[74] However, the outer structures in the present 25-keV collisions cannot be interpreted as either noise or artifacts of the calculations because the magnitudes of such density oscillations are quite outside the error limits for the present consistent and stable calculations. Also, such structures were not found during the forward and backward propagation of the soliton pulse, using the same algorithm. Note also that in relatively low-energy α-H collisions (1-keV) density plots do not reveal any noise.[74]

Since a TFD-like profile of the radial density persists over the time steps considered, there arises the interesting possibility of a solitary-wave solution to Eq. (13). In other words, although there arises strong density oscillations when the proton approaches the target Ne atom more closely, the envelope over these fluctuations may be a solitary wave.[71,72] This can happen if the strong dispersive effect of the Laplacian operator is counterbalanced by the highly nonlinear effective potential in Eq. (13). A definite conclusion on this requires a detailed mathematical analysis which is beyond the scope of the present work.

2. *Time-dependent effective potential*

From Fig. 4, one can discern *three* distinct zones in v_{eff}, viz. an attractive zone (negative v_{eff}) near the Ne nucleus, then a repulsive zone (positive v_{eff}), followed by another attractive zone (negative v_{eff}). The occurrence of these zones and their relative movement over a course of time are consequences of the density-dependent attractive and repulsive terms in v_{eff} in Eq. (14). The logarithmic plots show discontinuities at the boundaries separating the different zones. Two main aspects of the time evolution of v_{eff} are the following. (i) The r values separating the three zones oscillate in a nonlinear way. The inner and outer parts oscillate differently; sometimes they move in opposite directions and sometimes in the same direction. (ii) The entire potential curve oscillates (pulsating potential). Such nonlinear perturbations of the target atom density by the incoming proton may be explained as follows: as the proton approaches the target Ne atom, the outer "loosely bound" part of the electron density tends to gravitate towards the proton. As a consequence, the inner electron density is inadequately screened from the Ne nucleus and tends to accumulate near the nucleus. Charge accumulation in these two regions is accompanied by charge depletion in the intermediate region in order to preserve normalization. This picture is consistent with the fact that electronic charge tends to flow into the regions of negative (attractive) potential and flow away from a region of positive (repulsive) potential. Of the two largest dips in the effective potential plots, the first corresponds to the inner part of the radial density (see also Fig. 3). Note again that the three potential zones oscillate as the interaction gradually builds up. The oscillations of the two attractive zones may be likened to those of a set of two nonlinear coupled oscillators. Table II gives the radial density and effective potential at the 61st time step as functions of r.

It is worthwhile to make a comment on the possibility of solitary-wave (or soliton) solution of Eq. (13). In the usual cubic NLSE,

$$i\psi_t + \tfrac{1}{2}\psi_{xx} - \sigma|\psi|^2\psi = 0 , \tag{75}$$

where the subscripts denote partial differentiation, the repulsive interaction ($\sigma > 0$) gives rise to modulational stability[75] in which any initial data that vanish as $|x| \to \infty$ evolve into decaying oscillations whereas a soliton solution results in the case of modulational instability ($\sigma < 0$). If we write Eq. (13) as

$$i\psi_t + \tfrac{1}{2}\psi_{xx} - \frac{v_{\text{eff}}}{\rho}|\psi|^2\psi = 0 , \tag{76}$$

where v_{eff}/ρ plays the role of σ and compare Eq. (76) with Eq. (75) then, ρ being always positive, the negative values of v_{eff} are capable of yielding a soliton solution. The persisting crownlike structure in the radial density may be due to the repulsive zone of v_{eff} causing a "modulational stability."

C. Solution in two spatial dimensions

The target Ne nucleus is placed at the center of cylindrical polar coordinates, $0 \leq \tilde{\rho} \leq \infty$, $-\infty \leq z \leq \infty$, for a proton-neon headon ($b=0$) collision. (See Table III.) As in the one-dimensional case, $v_p = 1$ a.u., i.e., proton energy is 25 keV. The azimuthal angle $0 \leq \tilde{\phi} \leq 2\pi$ has been averaged out. Equation (13) is then solved by using an alternating direction implicit (ADI) version[65] of the Crank-Nicolson FD scheme, to calculate TD charge density, current density, effective potential, and chemical potential. The electronic part of the TD-induced dipole moment is calculated as (see Table III)

$$\mu_{\text{ind}}(t) = \int z\rho(\mathbf{r},t)d\mathbf{r} \ . \tag{77}$$

Using the transformations

$$y = \tilde{\rho}\phi \ , \tag{78}$$

$$\tilde{\rho} = x^2 \ , \tag{79}$$

Eq. (13) assumes the form

$$i\left[-\frac{3}{4x^3}\frac{\partial y}{\partial x}+\frac{1}{4x^2}\frac{\partial^2 y}{\partial x^2}+\frac{\partial^2 y}{\partial z^2}\right]+i\left[\frac{1}{x^4}-2v_{\text{eff}}\right]y = 2\frac{\partial y}{\partial t} \ . \tag{80}$$

Equation (80) is an initial boundary value problem which has been solved by the ADI method using the following set of boundary conditions:

At $t=0$, $y(x,z)$ is known $\forall x,z$

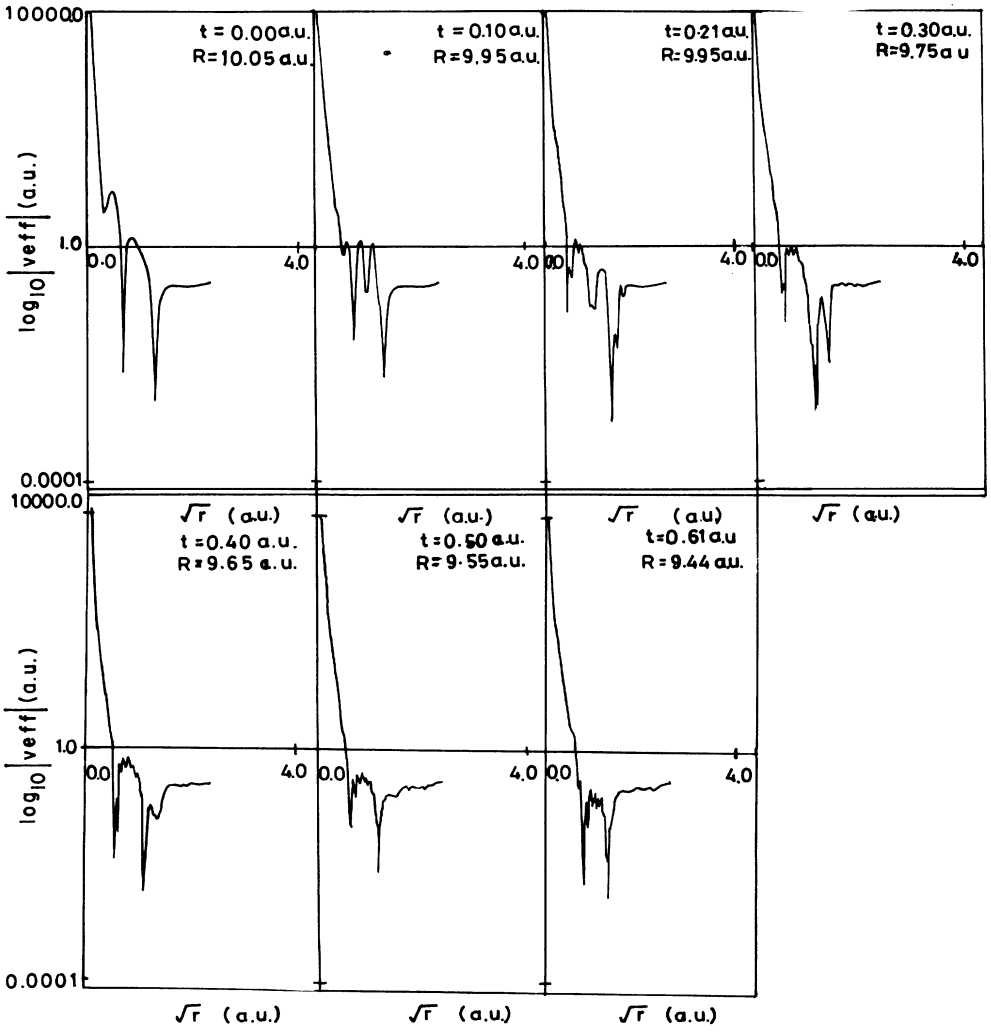

FIG. 4. Multiwindow plot of $\log_{10}|v_{\text{eff}}|$ against $\sqrt{r}$ for the proton-neon scattering system ($v_p=1$, $b=1$ a.u.) up to 61 time steps, in the spherically symmetric approximation.

TABLE II. Radial density and effective potential of the proton-neon atom scattering system, in the spherically symmetric approximation, as functions of r. Here $t=0.61$, $R=9.44$, proton velocity is equal to 1, impact parameter is equal to 1. The input density profile for a Ne atom at $t=0$ was taken from Clementi and Roetti (Ref. 70). All values are in atomic units.

r	$4\pi r^2\rho$	v_{eff}
0.0004	7.889×10^{-5}	-1.229×10^{6}
0.0400	4.007	-1.860×10^{2}
0.1521	8.828	−8.604
0.1764	8.699	−6.715
0.2209	9.213	−2.871
0.2704	8.599	−2.201
0.3025	8.766	−1.134
0.3844	8.124	−0.473
0.5041	7.228	−0.0319
0.5184	7.167	0.0260
0.7396	5.786	0.235
1.0201	4.281	0.164
1.4641	2.671	2.62×10^{-3}
1.4884	2.526	-2.061×10^{-2}
1.8769	1.283	−0.179
2.6244	0.626	−0.221
4.4944	3.715×10^{-3}	−0.236
4.5369	1.682×10^{-2}	−0.248
5.6169	0.163	−0.314
5.7600	0.0315	−0.310

(input density near-Hartree-Fock,[70] Dirichlet data)

$$y(0,z)=0=y(\infty,z),\quad \forall z,t\ ,$$
$$y(x,\pm\infty)=0,\quad \forall x,t\ . \tag{81}$$

In the ADI approach, the FD equations are written in terms of quantities at two different time steps. Two different FD approximations are used alternately: the first advances the calculation from the nth to the $(n+1)$th time step while the second advances the calculation from the $(n+1)$th to the $(n+2)$th time step. The second approximation does not require any information about values at the nth time step. The first approximation is obtained by replacing all x derivatives by Crank-Nicolson analogues and z derivatives by an explicit scheme. Taking N to be the number of steps in the direction (either x or z, in turn) in which the implicit scheme is used, the solution of the resulting $(N-1)$ unknowns per line in the $(N-1)$ equations can be obtained at the $(n+1)$th time step via the tridiagonal Thomas algorithm. The second approximation is obtained by reversing the Crank-Nicolson-explicit terms and using the Thomas algorithm again. Thus, the solution to Eq. (80) is obtained by alternating between rows and columns in the (x,z) space and then solving tridiagonal equations.

TABLE III. Time-dependent electronic induced dipole moment along the internuclear axis of a Ne atom being approached by a proton in a straight line for a headon collision. The proton velocity is equal to 1, impact parameter $b=0$; R is the internuclear distance. All values are in atomic units.

Time	R	μ_{ind}
0	10.0	0
0.02	9.98	0.0058
0.04	9.96	0.055
0.06	9.94	−0.439
0.08	9.92	0.425

The integral in the screened nuclear charge Q, given in Eq. (15) has been calculated in the following manner. The Coulomb repulsion potential $\{|\mathbf{r}-\mathbf{r}'|\}^{-1}$ can be considered as the Green's function of the Laplacian operator. In cylindrical polar coordinates $(z,\tilde{\rho},\tilde{\phi})$ it is given by[76]

$$\frac{1}{|\mathbf{r}-\mathbf{r}'|}=\sum_{m=0}^{\infty}\epsilon_m\cos[m(\tilde{\phi}-\tilde{\phi}')]\times\int_0^{\infty}J_m(k\tilde{\rho})J_m(k\tilde{\rho}')\times\exp\{-k|z-z'|\}dk\ , \tag{82}$$

$\epsilon_0=1,\epsilon_m=2$ for $m=1,2,3,\ldots$.

After integrating over $0\le\tilde{\phi}\le2\pi$, the only nonvanishing term from the above infinite series is that with $m=0$. The final numerical integration has been done according to Gauss-Legendre quadrature. This entire procedure was tested by calculating the Coulomb energy of the Ne atom; our calculated value was 244.6 a.u., in comparison with the Hartree-Fock value of 245.1 a.u.

An effective alternative (not employed in these calculations) to the expansion (82) is to employ an integral transform, viz. either

$$\frac{1}{|\mathbf{r}-\mathbf{r}'|}=\frac{1}{\sqrt{\pi}}\int_0^{\infty}ds\,s^{-1/2}\exp(-s|\mathbf{r}-\mathbf{r}'|^2) \tag{83a}$$

or

$$\frac{1}{|\mathbf{r}-\mathbf{r}'|}=\int_0^{\infty}ds\,\exp(-s|\mathbf{r}-\mathbf{r}'|)\ . \tag{83b}$$

By interpolating the TD density $\rho(\mathbf{r},t)$ in terms of Gaussian-type functions in the case of (83a) and Slater-type functions in the case of (83b), it is possible to evaluate most of the integrals analytically. The basic integrals need to be calculated at only one instant of time; at all other times, only the interpolating coefficients change and are to be determined separately.

The overall two-step ADI approach requires minimal computer storage and is quite accurate. The truncation error is $O\{(\Delta x)^2\}$, $O\{(\Delta z)^2\}$, and $O\{(\Delta t)^2\}$. The two-step scheme is unconditionally stable and consistent[73] with the parabolic partial differential equation (80).

The final set of difference equations for the first approximation (x direction) for any mesh point in t and for a particular m may be written as

$$c_l y_{l-1,m}^{n+1}+a_l y_{l,m}^{n+1}+b_l y_{l+1,m}^{n+1}=d_l\ , \tag{84a}$$

where $l=1,2,\ldots,L$; $m=1,2,\ldots,M$; $c_1=b_L=0$; L is the number of mesh points in x and M is the number of mesh points in z.

In Eq. (84a), the quantities a,b,c,d are given by

$$c_l = \left[-\frac{3}{16x_1^3}\frac{i}{\Delta x} - \frac{1}{8x_1^2}\frac{i}{(\Delta x)^2} \right] , \tag{84b}$$

$$a_l = \left[\frac{i}{4x_1^2(\Delta x)^2} + \frac{2}{\Delta t} + i\left\{ v_{\text{eff}} - \frac{1}{2x_1^4} \right\} \right] , \tag{84c}$$

$$b_l = \left[\frac{3}{16x_1^3}\frac{i}{\Delta x} - \frac{1}{8x_l^2}\frac{i}{(\Delta x)^2} \right] , \tag{84d}$$

$$d_l = -\frac{3i}{8x_l^3}\left[\frac{\partial y}{\partial x}\right] + \frac{i}{8x_1^2}\left[\frac{\partial^2 y}{\partial x^2}\right] + i\left[\frac{\partial^2 y}{\partial z^2}\right] - \left[i\left[v_{\text{eff}} - \frac{1}{2x_l^2} \right] - \frac{2}{\Delta t} \right] y_{l,m}^n . \tag{84e}$$

The various derivatives in Eq. (84e) have been calculated by using their explicit forms, viz.

$$\left[\frac{\partial y}{\partial x}\right] = \frac{y_{l+1,m}^n - y_{l-1,m}^n}{2\Delta x} , \tag{85a}$$

$$\left[\frac{\partial^2 y}{\partial x^2}\right] = \frac{y_{l+1,m}^n - 2y_{l,m}^n + y_{l-1,m}^n}{(\Delta x)^2} , \tag{85b}$$

$$\left[\frac{\partial^2 y}{\partial z^2}\right] = \frac{y_{l,m+1}^n - 2y_{l,m}^n + y_{l,m-1}^n}{(\Delta z)^2} . \tag{85c}$$

In Eqs. (84) and (85), Δx, Δz, and Δt are the step sizes in x, z, and t, respectively; l,m,n denote the mesh points in x, z, t, respectively. Here, $\Delta x = \Delta z = \Delta t = 0.01$ a.u.

The following tridiagonal matrix equation is solved by using a modified Thomas algorithm and the boundary conditions (81):

$$\begin{bmatrix} a_1 & b_1 & & & \\ c_2 & a_2 & b_2 & & [0] \\ & \ddots & \ddots & \ddots & \\ [0] & & \ddots & \ddots & b_{L-1} \\ & & & c_L & a_L \end{bmatrix} \begin{bmatrix} y_i \\ y_2 \\ \vdots \\ \vdots \\ y_L \end{bmatrix} = \begin{bmatrix} d_1 \\ d_2 \\ \vdots \\ \vdots \\ d_L \end{bmatrix} . \tag{86}$$

A near-Hartree-Fock trial solution is used as the initial input in order to launch the process of solution. After solving Eq. (86), we obtain $\{y_{l,m}^{n+1}\}$ which is taken as the trial solution for the second approximation where z derivatives are replaced by their Crank-Nicolson forms and the x derivatives are obtained via the explicit sheme.

In case of the second approximation (z direction), the difference equations for a particular l are

$$c_m y_{l,m-1}^{n+2} + a_m y_{l,m}^{n+2} + b_m y_{l,m+1}^{n+2} = d_m, \ldots , \tag{87a}$$

$$c_1 = b_M = 0 ,$$

where

$$c_m = -\frac{i}{2(\Delta z)^2} , \tag{87b}$$

$$a_m = \left[\frac{i}{(\Delta z)^2} + i\left\{ v_{\text{eff}} - \frac{1}{2x_l^4} \right\} + \frac{2}{\Delta t} \right] , \tag{87c}$$

$$b_m = -\frac{i}{2(\Delta z)^2} , \tag{87d}$$

$$d_m = -\frac{3i}{4x_l^3}\left[\frac{\partial y}{\partial x}\right] + \frac{i}{4x_l^2}\left[\frac{\partial^2 y}{\partial x^2}\right] + \frac{i}{2}\left[\frac{\partial^2 y}{\partial z^2}\right] - \left[i\left\{ v_{\text{eff}} - \frac{l}{2x_l^4} \right\} - \frac{2}{\Delta t} \right] y_{l,m}^{n+1} . \tag{87e}$$

As before, the derivatives in Eq. (87e) are calculated in an explicit manner [see Eq. (85)].

Now, the following tridiagonal matrix equation is solved by employing the same modified Thomas algorithm and the boundary conditions (81):

$$\begin{bmatrix} a_1 & b_1 & & & \\ c_2 & a_2 & b_2 & & [0] \\ & \ddots & \ddots & \ddots & \\ [0] & & \ddots & \ddots & b_{M-1} \\ & & & c_M & a_M \end{bmatrix} \begin{bmatrix} y_1 \\ y_2 \\ \vdots \\ \vdots \\ y_M \end{bmatrix} = \begin{bmatrix} d_1 \\ d_2 \\ \vdots \\ \vdots \\ d_M \end{bmatrix} . \tag{88}$$

The solution of Eq. (88) completes the ADI cycle. For going to the next cycle, the solution of Eq. (88) is taken as the input.

After calculating $\{y_{l,m}^n\}$, we obtain the TD "wave function" ϕ from Eq. (78) and then calculate the TD density, potential, chemical potential, and induced dipole moment at a particular instant of time by employing Eqs. (8b), (14), (26), (37), and (77), respectively. The current density $\mathbf{j}$ is calculated as

$$\mathbf{j} = [\phi_{re}\nabla\phi_{im} - \phi_{im}\nabla\phi_{re}] . \tag{89}$$

Using (8a), one can readily show that, in a.u., $\mathbf{j} = \rho\mathbf{v} = \rho\nabla\chi$ is identical to the form given by Eq. (89).

D. Interpretation of two-dimensional results

The calculations pertain to the initial part of the approach regime, covering the ranges $t = 0$–0.08, $R = 10.0$–9.92 a.u. All quantities reported here are with reference to a state of no interaction at $t = 0$, $R = 10.0$ although, strictly speaking, the interaction does not vanish at $R = 10$. The induced dipole moment oscillates fairly rapidly and even changes its sign; such oscillations have earlier been reported by Horbatsch[42] and mainly indicate collective oscillations of the outer parts of neon's electron density. Figures 5–8 depict the perspective plots of TD v_{eff}, ρ, $|\mathbf{j}|$, and μ in a cylindrical polar coordinate mesh.

Figures 4 and 5 reveal structural similarities between the v_{eff} plots for the one- and two-dimensional cases. The oscillations of the entire pulsating potential surface now manifest themselves more clearly. The peaks (repulsive) and troughs (attractive) occur due to the relative magnitudes of the attractive and repulsive terms in v_{eff}. The

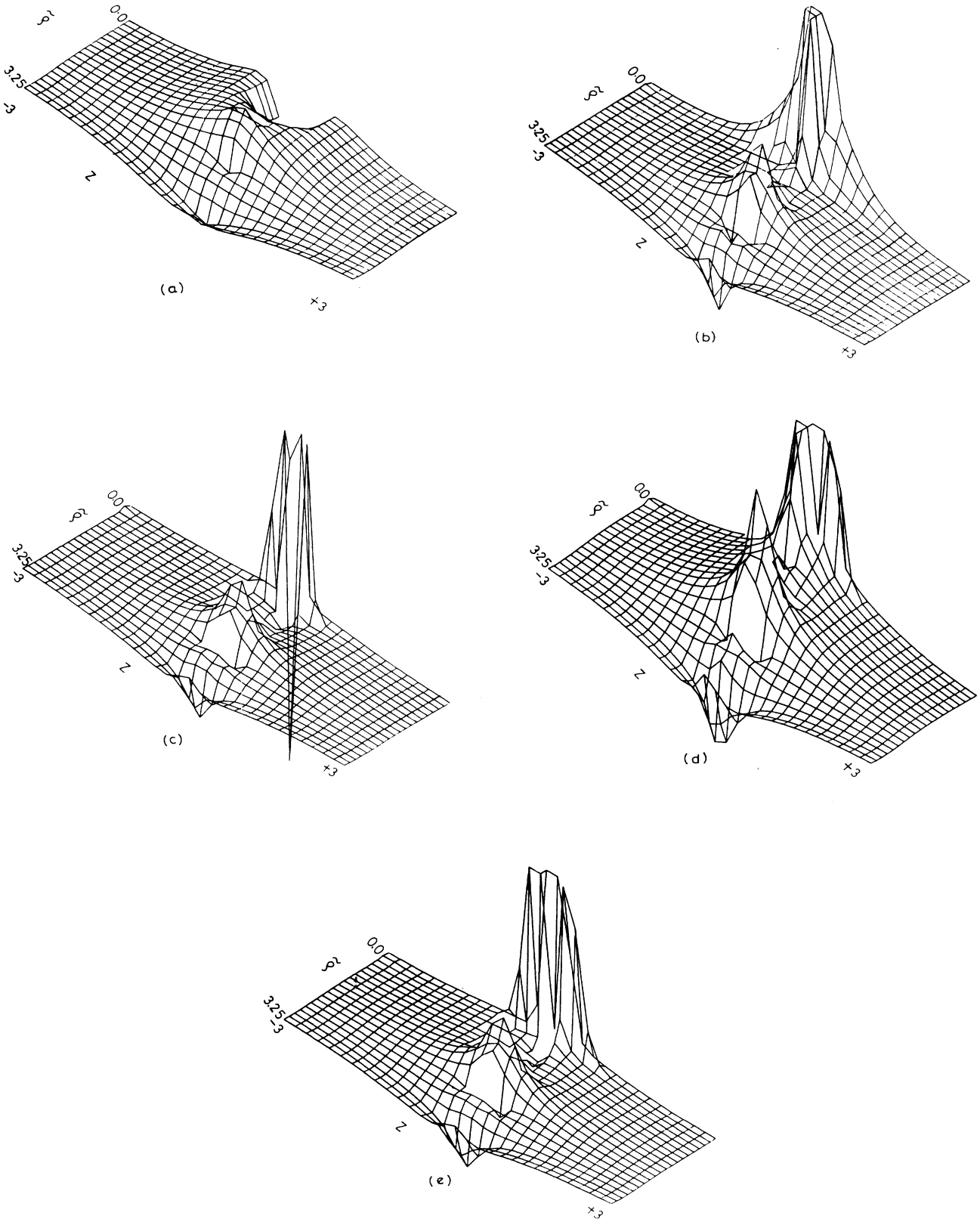

FIG. 5. Perspective plots (a.u.) of $-50 \leq v_{\text{eff}} \leq 50$ in the proton-neon scattering system ($v_p = 1$, $b = 0$ a.u.) in cylindrical polar coordinates $(\tilde{\rho}, z)$. The basal rectangular mesh designates the $(\tilde{\rho}, z)$ plane, where $0 \leq \tilde{\rho} \leq 3.25$ and $-3 \leq z \leq 3$. The target Ne nucleus is at (0,0) and the proton is approaching from the left along the $\tilde{\rho} = 0$ direction of z. (a) $t = 0, R = 10.0$; (b) $t = 0.02, R = 9.98$; (c) $t = 0.04, R = 9.96$; (d) $t = 0.06, R = 9.94$; (e) $t = 0.08, R = 9.92$.

ranges as well as heights (depths) of these peaks (troughs) oscillate from $t=0-0.08$. At $t=0$ [Fig. 5(a)] there is an infinite trough (negative, attractive v_{eff}) at the Ne nuclear site; along the $\tilde{\rho}$ direction, corresponding to $z=0$, this trough is followed by a peak (positive, repulsive v_{eff}) and a trough. From $t=0.02$ onwards, the infinite trough [generally masked in Figs. 5(b)–5(e)] at the nuclear site is followed by two peaks and an outer trough. During these eight time steps, the positions of these peaks and troughs do not change significantly. For a given $\tilde{\rho}$, along the z direction, the oscillations of the highest peak are quite noticeable. At $\tilde{\rho}=0$, on both sides of $z=0$, v_{eff} passes from an attractive to a repulsive zone before plunging into the trough at the nuclear site. Since the proton is approaching from the left, the peaks and troughs have a somewhat asymmetrical shape. Table IV gives the values

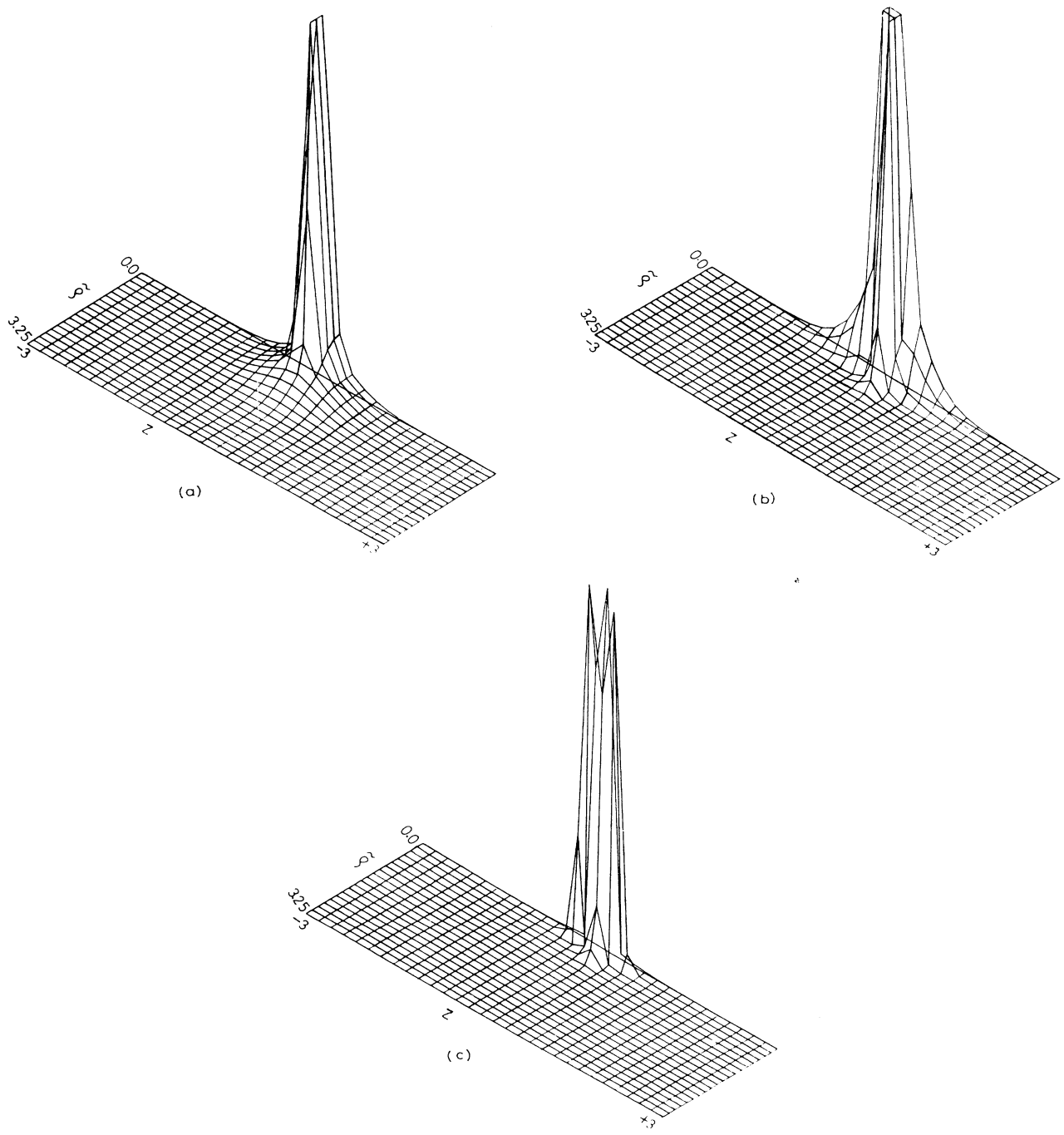

FIG. 6. Perspective plots (a.u.) of $0 \le \rho \le 50$ in the proton-neon scattering system ($v_p=1, b=0$ a.u.) in cylindrical polar coordinates $(\tilde{\rho},z)$; see caption of Fig. 5 for other details.

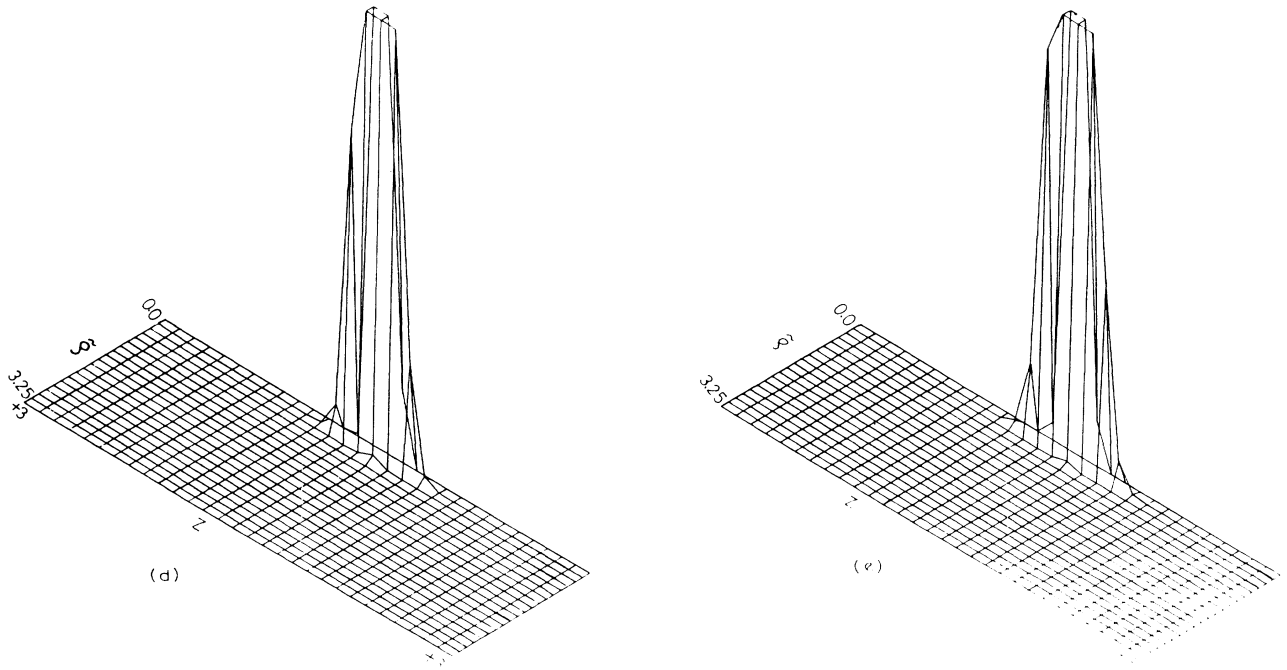

FIG. 6. (*Continued*).

of v_{eff} for a range of $\tilde{\rho}$ and z, at $t=0.08$.

Interestingly, the $\tilde{\rho}$-dependent structure of v_{eff} does not appear to be manifested so clearly in the perspective plots of ρ [Figs. 6(a)–6(e)] and $|\mathbf{j}|$ [Figs. 7(a) and 7(b)]. For both of these quantities the effective diameter of the cylinder appears smaller than that of v_{eff}. However, both ρ and $|\mathbf{j}|$ show prominent collective oscillations, particularly in the outer regions, along the z direction. As in the one-dimensional case, the attractive zones in v_{eff} tend to cause an accumulation of electronic charge in these zones whereas the repulsive zones tend to cause a depletion of electronic charge. It is worthwhile to note that the

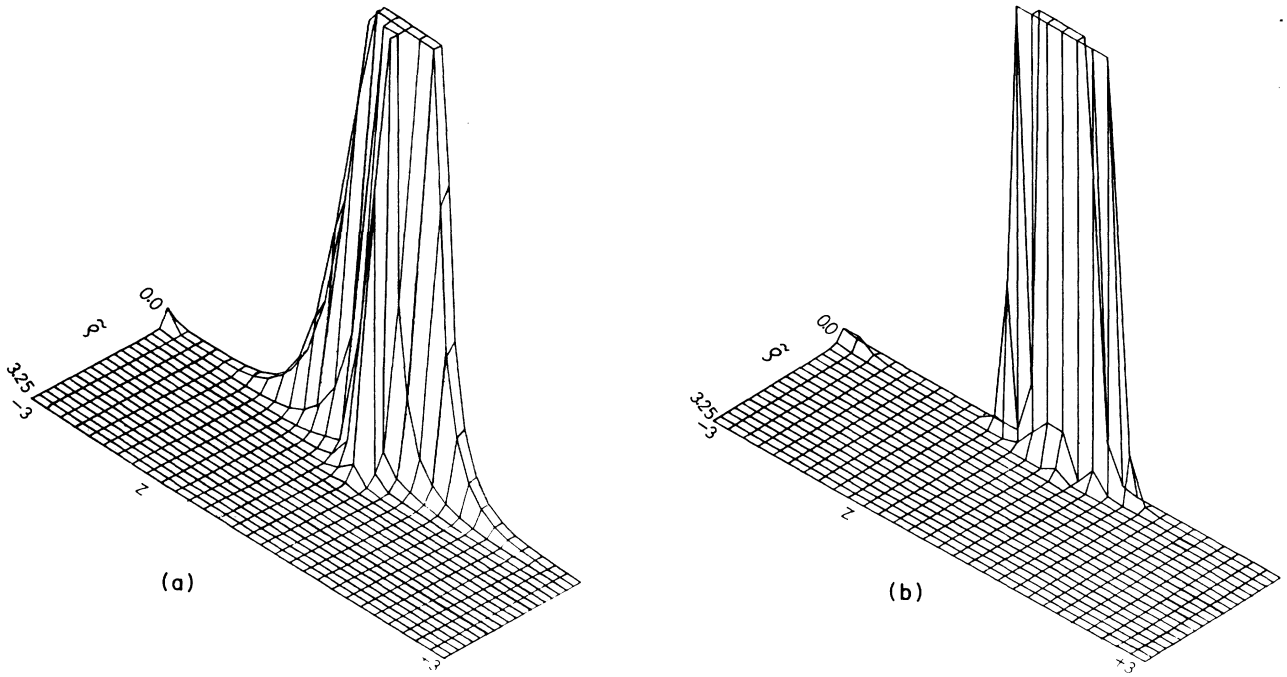

FIG. 7. Perspective plots (a.u.) of $0 \leq |\mathbf{j}| \leq 50$ in the proton-neon scattering system ($v_p=1, b=0$ a.u.) in cylindrical polar coordinates $(\tilde{\rho}, z)$. Here (a) $t=0.02, R=9.98$; (b) $t=0.08, R=9.92$; see caption of Fig. 5 for other details.

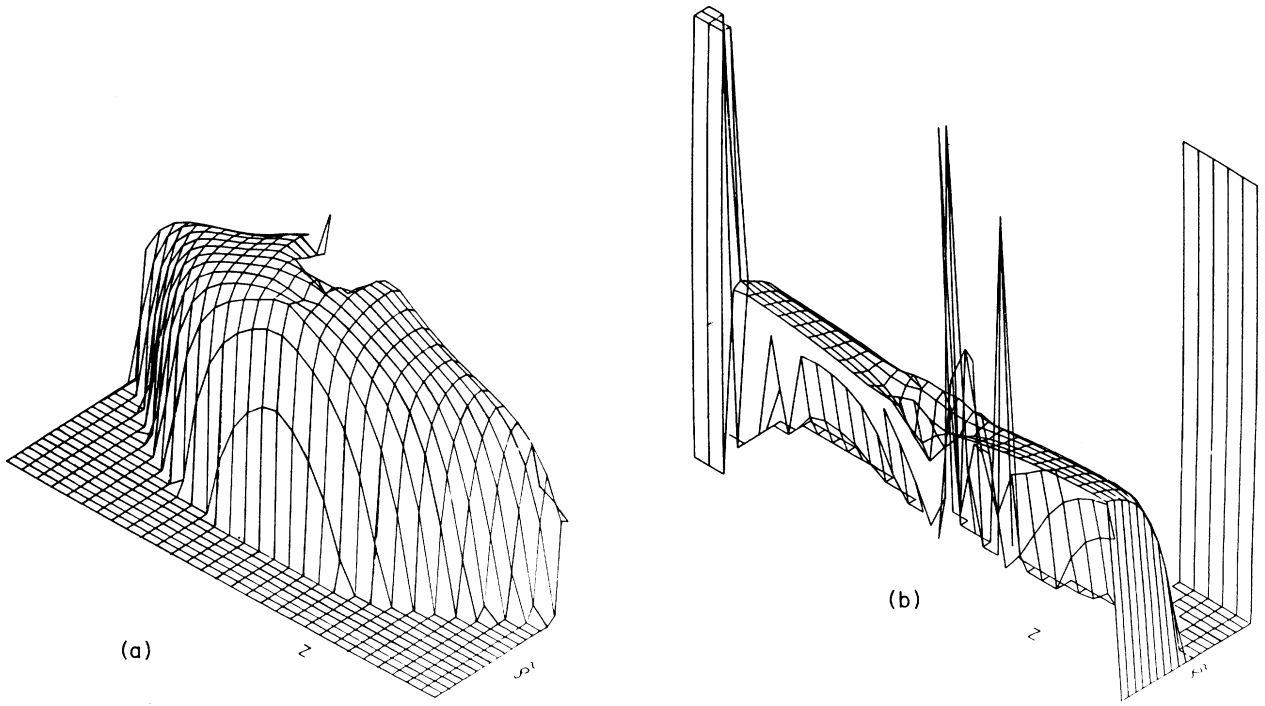

FIG. 8. Perspective plots (a.u.) of $-50 \leq \mu \leq 50$ in the proton-neon scattering system ($v_p = 1, b = 0$ a.u.) in cylindrical polar coordinates $(\tilde{\rho}, z)$. Here (a) $t = 0, R = 10.0$; (b) $t = 0.08, R = 9.92$; see caption of Fig. 5 for other details.

current density $\mathbf{j}$ is nonvanishing because as the proton approaches the Ne atom, excited states of the latter start mixing with the ground state. Table V gives the values of ρ and $|\mathbf{j}|$ for a range of $\tilde{\rho}$ and z at $t = 0.08$.

The most striking variations are observed in the perspective plots [Figs 8(a) and 8(b)] of the space-time-dependent chemical potential, $\mu(\mathbf{r}, t)$, obtained from the calculated $\rho(\mathbf{r}, t)$. However, it is difficult to interpret these plots. Clearly, since μ undergoes such dramatic changes, it should be a very useful quantity for monitoring a TD process. Techniques for interpreting such complicated oscillating structures in $\mu(\mathbf{r}, t)$ are to be developed. In particular, the accordion structure at $t = 0$ seems to occur because (i) at $R = 10$, the interaction is not zero as we have assumed, (ii) the approximate KED functional employed in this work leads to a v_{eff} which yields a space-dependent chemical potential, instead of a constant as one expects in ground-state DFT, due to unbalanced terms in Eq. (37). As time progresses, the accordion structure gradually disappears to give rise to a somewhat "chaotic" pattern. Table IV gives the values of $\mu(\mathbf{r}, t)$ for a range of $\tilde{\rho}$ and z at $t = 0.08$.

TABLE IV. Effective potential (v_{eff}) and chemical potential (μ) in the cylindrically symmetrical proton-neon scattering system as functions of the cylindrical coordinates $\tilde{\rho}$ and z. Here, $t = 0.08$, $R = 9.92$, proton velocity is equal to 1, impact parameter is equal to 0. The initial ($t = 0$) near-Hartree-Fock input density for Ne was taken from Clementi and Roetti (Ref. 70). All values are in atomic units. For every $(\tilde{\rho}, z)$ the set of two values corresponds to v_{eff} and μ from top to bottom.

	$\tilde{\rho}$				
z	0.09	0.3025	0.64	1.69	3.24
−2.0	−1.595	−1.618	−1.718	−2.572	−3.980
	-0.6570×10^{7}	-0.217×10^{4}	-0.1166×10^{3}	−15.80	−6.814
−0.5	0.7627	0.3796	0.5254	0.7320	−9.686
	-0.4275×10^{6}	-0.5164×10^{8}	-0.6124×10^{5}	−28.75	−12.61
0.0	−26.77	−1.789	3.820	12.05	−21.48
	0.6061×10^{3}	-0.1357×10^{5}	-0.5909×10^{8}	−24.30	−24.68
0.5	2.896	1.688	0.8916	1.103	−10.20
	-0.4749×10^{6}	-0.5371×10^{8}	-0.5760×10^{5}	−31.27	−13.12
2.0	−1.420	−1.447	−1.561	−2.504	−4.040
	-0.2063×10^{7}	-0.2372×10^{4}	-0.1152×10^{3}	−15.72	−6.875

TABLE V. Charge density (ρ) and current density ($|\mathbf{j}|$) in the cylindrically symmetrical proton-neon scattering system as functions of the cylindrical coordinates $\tilde{\rho}$ and z. Here $t=0.08$, $R=9.92$, proton velocity is equal to 1, impact parameter is equal to 0. The initial ($t=0$) near-Hartree-Fock input density for Ne was taken from Clementi and Roetti (Ref. 70). All values are in atomic units. For every $(\tilde{\rho},z)$ the set of two values corresponds to ρ and $|\mathbf{j}|$ from top to bottom.

	$\tilde{\rho}$	
z	0.09	0.3025
−0.5	0.01133	0.2381×10^{-5}
	1.168	0.6978×10^{-4}
0.0	0.4699	0.00176
	11.41	0.03179
0.5	0.01311	0.2550×10^{-5}
	1.389	0.7601×10^{-4}

V. CONCLUSION

The new features in the present study of ion-atom collisions may be summarized as follows.

(i) Simultaneous incorporation of the three main problems facing present-day DFT, viz. kinetic energy, excited states, and time dependence.

(ii) An interlinking of DFT and QFD to follow a TD process from "start" to "finish" in terms of an SDE.

(iii) The use of a new KED functional which seems to be the best practical compromise so far.

(iv) The derivation of a TDSDE for direct calculation of charge density and current density, i.e., both the amplitude and the phase of a single "orbital" for the many-electron system.

(v) The concept of a TD (pulsating) effective potential surface on which the process occurs and the concept of a space-time-dependent chemical potential.

(vi) The TDSDE is a new GNLSE and might govern a range of dynamical processes in quantum chemistry. A study of the integrability and other mathematical properties (e.g., quantum solitons or solitary waves or quantum chaos) would be of interest.

(vii) Incorporation of Nelson's stochastic mechanics into the DFT-QFD framework.

(viii) Explicit manifestation of nonlinearity, if present, in molecular scattering processes.

(ix) A new algorithm for the numerical solution of the present GNLSE.

(x) Perspective plots of TD density, current density, effective potential, and chemical potential for a quantum process. To our knowledge, such plots of the first three quantities were first given by Kreuzer[77,78] in a statistical-mechanical and fluid-dynamical treatment of the time evolution of an ideal gas in an external potential. Dynamical electron current induced by molecular vibration has also been depicted by Tachibana *et al.*[79] in a different context.

It is hoped that our attempt to interlink all the above features into a consistent framework might lend additional support to "classical" interpretations of quantum mechanics. A preliminary report of this work is given in Ref. 80.

ACKNOWLEDGMENTS

We thank Dr. S. Rao Koneru, Professor S. K. Malik, Professor G. Govil, and Dr. A. Saran for their help in various ways. Thanks are also due to the Council of Scientific and Industrial Research, New Delhi, for financial support and the Panjab University, Chandigarh, for a computation grant.

APPENDIX: DERIVATION OF THE TDSDE, EQ. (13) WITHIN A QFDFT

Consider Eqs. (2)–(4) and (6)–(12). From Eq. (8), one obtains

$$\nabla\rho=\rho\left[\frac{2\nabla\phi}{\phi}-2i\nabla\chi\right], \tag{A1a}$$

$$\nabla^2\rho=\rho\left[\frac{2(\nabla\phi)^2}{\phi^2}+\frac{2\nabla^2\phi}{\phi}-\frac{8i\nabla\phi\cdot\nabla\chi}{\phi}-4(\nabla\chi)^2-2i\nabla^2\chi\right], \tag{A1b}$$

$$\frac{\partial\rho}{\partial t}=\rho\left[2\frac{(\partial\phi/\partial t)}{\phi}-2i\frac{\partial\chi}{\partial t}\right]. \tag{A1c}$$

Using Eqs. (2)–(4) and (9)–(11) leads to

$$\frac{\delta G}{\delta\rho}=\tfrac{5}{3}C_k\rho^{2/3}+\frac{1}{8}\left[\left[\frac{\nabla\rho}{\rho}\right]^2-2\frac{\nabla^2\rho}{\rho}\right]-\frac{a(N)}{r^2}+\frac{f(R,N)}{N}-\tfrac{4}{3}C_x\rho^{1/3}. \tag{A2a}$$

Substituting the expressions for $\nabla\rho$ and $\nabla^2\rho$ from (A1) into (A2a) the latter becomes

$$\frac{\delta G}{\delta\rho}=\tfrac{5}{3}C_k\rho^{2/3}+\left[\tfrac{1}{2}(\nabla\chi)^2-\frac{1}{2}\frac{\nabla^2\phi}{\phi}+\frac{i\nabla\phi\cdot\nabla\chi}{\phi}+\frac{i}{2}\nabla^2\chi\right]-\frac{a(N)}{r^2}+\frac{f(R,N)}{N}-\tfrac{4}{3}C_x\rho^{1/3}. \tag{A2b}$$

Equations (7) and (A2b) together lead to

$$\frac{\partial\chi}{\partial t}+(\nabla\chi)^2-\frac{1}{2}\frac{\nabla^2\phi}{\phi}+\frac{i\nabla\phi\cdot\nabla\chi}{\phi}+\frac{i}{2}\nabla^2\chi+\tfrac{5}{3}C_k\rho^{2/3}-\frac{a(N)}{r^2}+\frac{f(R,N)}{N}-\tfrac{4}{3}C_x\rho^{1/3}+\int\frac{\rho(\mathbf{r}',t)}{|\mathbf{r}-\mathbf{r}'|}d\mathbf{r}'+v(\mathbf{r},t)=0,$$

i.e.,

$$\frac{\partial\chi}{\partial t}=-(\nabla\chi)^2+\frac{1}{2}\frac{\nabla^2\phi}{\phi}-\frac{i\nabla\phi\cdot\nabla\chi}{\phi}-\frac{i}{2}\nabla^2\chi-v_{\text{eff}}(\mathbf{r},t), \tag{A3a}$$

where

$$v_{\text{eff}}(\mathbf{r},t)=\tfrac{5}{3}C_k\rho^{2/3}-\frac{a(N)}{r^2}+f(R,N)/N-\tfrac{4}{3}C_x\rho^{1/3}+\int\frac{\rho(\mathbf{r}',t)}{|\mathbf{r}-\mathbf{r}'|}d\mathbf{r}'+v(\mathbf{r},t)\ . \tag{A3b}$$

On the other hand, Eqs. (6) and (A1c) together give rise to

$$\rho\left[2\frac{(\partial\phi/\partial t)}{\phi}-2i\frac{\partial\chi}{\partial t}\right]=-\nabla\cdot(\rho\nabla\chi)=-\rho\left[\nabla^2\chi+2\frac{\nabla\phi\cdot\nabla\chi}{\phi}-2i(\nabla\chi)^2\right],$$

i.e.,

$$\left[2\frac{(\partial\phi/\partial t)}{\phi}-2i\frac{\partial\chi}{\partial t}\right]=-\left[\nabla^2\chi+\frac{2\nabla\phi\cdot\nabla\chi}{\phi}-2i(\nabla\chi)^2\right]. \tag{A4}$$

Substituting the expression for $\partial\chi/\partial t$ from Eq. (A3a) into Eq. (A4), we obtain

$$\left[2\frac{(\partial\phi/\partial t)}{\phi}+2i(\nabla\chi)^2-i\frac{\nabla^2\phi}{\phi}-\frac{2\nabla\phi\cdot\nabla\chi}{\phi}-\nabla^2\chi+2iv_{\text{eff}}(\mathbf{r},t)\right]=-\left[\nabla^2\chi+\frac{2\nabla\phi\cdot\nabla\chi}{\phi}-2i(\nabla\chi)^2\right],$$

i.e.,

$$\left[2\frac{(\partial\phi/\partial t)}{\phi}-i\frac{\nabla^2\phi}{\phi}+2iv_{\text{eff}}(\mathbf{r},t)\right]=0\ . \tag{A5}$$

It is interesting to note that if one considers any multiple of $T_w[\rho]$ in the KE functional the above cancellations do not occur. This indicates the importance of the full Weizsäcker term. Equation (A5), on rearrangement, yields the TDSDE (13).

[1] *Electron and Magnetization Densities in Molecules and Crystals,* edited by P. Becker (Plenum, New York, 1980).
[2] *The Force Concept in Chemistry,* edited by B. M. Deb (Van Nostrand-Reinhold, New York, 1981).
[3] *Electron Distributions and the Chemical Bond,* edited by P. Coppens and M. B. Hall (Plenum, New York, 1982).
[4] S. Fliszár, *Charge Distributions and Chemical Effects* (Springer-Verlag, Berlin, 1983).
[5] *Density Functional Theory,* Vol. 187 of *Lecture Notes in Physics,* edited by J. Keller and J. L. Gazquez (Springer-Verlag, Berlin, 1983).
[6] *Theory of the Inhomogeneous Electron Gas,* edited by S. Lundqvist and N. H. March (Plenum, New York, 1983).
[7] *Local Density Approximations in Quantum Chemistry and Solid State Physics,* edited by J. P. Dahl and J. Avery (Plenum, New York, 1984).
[8] *Density Functional Methods in Physics,* edited by R. M. Dreizler and J. da Providencia (Plenum, New York, 1985).
[9] *Density Matrices and Density Functionals,* edited by R. M. Erdahl and V. H. Smith, Jr. (Reidel, Dordrecht, 1987).
[10] E. S. Kryachko and E. V. Ludena, *Density Functional Theory in Quantum Chemistry* (Reidel, Dordrecht, 1987).
[11] *Single-Particle Density in Physics and Chemistry,* edited by N. H. March and B. M. Deb (Academic, London, 1987).
[12] A. S. Bamzai and B. M. Deb, Rev. Mod. Phys. **53**, 95 (1981); **53**, 593 (1981).
[13] R. F. W. Bader, T. T. Nguyen-Dang, and Y. Tal, Rep. Prog. Phys. **44**, 893 (1981).
[14] D. D. Koelling, Rep. Progr. Phys. **44**, 139 (1981).
[15] S. K. Ghosh and B. M. Deb, Phys. Rep. **92**, 1 (1982).
[16] R. G. Parr, Ann. Rev. Phys. Chem. **34**, 631 (1983).
[17] B. M. Deb and S. K. Ghosh, J. Chem. Phys. **77**, 342 (1982); L. J. Bartolotti, Phys. Rev. A **26**, 2243 (1982).
[18] H. Singh and B. M. Deb, Pramana **27**, 337 (1986).
[19] B. M. Deb and S. K. Ghosh, J. Phys. B **12**, 3857 (1979).
[20] B. M. Deb, in Ref. 7, p. 75.
[21] S. K. Ghosh and B. M. Deb, Int. J. Quant. Chem. **22**, 871 (1982).
[22] S. K. Ghosh and B. M. Deb, J. Phys. A **17**, 2463 (1984).
[23] B. M. Deb and P. K. Chattaraj, in *Solitons: Introduction and Applications,* edited by M. Lakshmanan (Springer-Verlag, Berlin, 1988); B. M. Deb and P. K. Chattaraj, Proc. Indian Acad. Sci. **99**, 67 (1987).
[24] B. M. Deb, Proc. Indian Nat. Sci. Acad. **54A**, 844 (1988).
[25] G. P. Lawes and N. H. March, Phys. Scr. **21**, 402 (1980); N. H. March, Phys. Lett. **A113**, 476 (1986).
[26] B. M. Deb and S. K. Ghosh, Int. J. Quant. Chem. **23**, 1 (1983).
[27] R. F. W. Bader and H. Essen, in Ref. 7, p. 129.
[28] M. Levy, J. P. Pardew, and V. Sahni, Phys. Rev. A **30**, 2745 (1984); M. Levy and H. Ou-Yang, *ibid.* **38**, 625 (1988).
[29] G. Hunter, Int. J. Quant. Chem. **29**, 197 (1986).
[30] E. Nelson, *Dynamical Theory of Brownian Motion* (Princeton University Press, Princeton, NJ, 1967).
[31] E. Nelson, *Quantum Fluctuations* (Princeton University Press, Princeton, NJ, 1985).
[32] G. C. Ghirardi, C. Omero, A. Rimini, and T. Weber, Riv. Nuovo Cimento **1**, 1 (1978).
[33] F. Guerra, Phys. Rep. **77**, 263 (1981).
[34] L. de la Pena and A. M. Cetto, Found. Phys. **12**, 1017 (1982).
[35] A. B. Nassar, J. Math. Phys. **27**, 755 (1986).
[36] J. C. Zambrini, Phys. Rev. A **33**, 1532 (1986).
[37] B. M. Deb and S. K. Ghosh, in Ref. 11, p. 219.
[38] H.-J. Lüdde, M. Horbatsch, E. K. U. Gross, and R. M. Dreizler, Proceedings of XVII International Winter Meeting on Nuclear Physics, Bormio, 1979 (unpublished), p. 120.
[39] M. Horbatsch and R. M. Dreizler, Z. Phys. A **300**, 119 (1981).
[40] M. Horbatsch and R. M. Dreizler, Z. Phys. A **308**, 329 (1982).
[41] P. Malzacher and R. M. Dreizler, Z. Phys. A **307**, 211 (1981).
[42] M. Horbatsch, J. Phys. B **16**, 4643 (1983).
[43] S. K. Ghosh and L. C. Balbas, J. Chem. Phys. **83**, 5778 (1985).
[44] S. Haq, P. K. Chattaraj, and B. M. Deb, Chem. Phys. Lett. **111**, 79 (1984); P. K. Chattaraj and B. M. Deb, *ibid.* **121**, 143 (1985).
[45] B. M. Deb and P. K. Chattaraj, Phys. Rev. A **37**, 4030 (1988).
[46] L. C. Snyder and H. Basch, *Molecular Wave Functions and Properties* (Wiley, New York, 1972).

[47]R. F. W. Bader, in Ref. 2, p. 39.
[48]Ch. V. Rama Rao and A. K. Chandra, Proc. Indian Acad. Sci. **96**, 195 (1986).
[49]P. K. Chattaraj and B. M. Deb, J. Sci. Ind. Res. **43**, 238 (1984).
[50]E. Runge and E. K. U. Gross, Phys. Rev. Lett. **52**, 997 (1984).
[51]B. X. Xu and A. K. Rajagopal, Phys. Rev. A **31**, 2682 (1985).
[52]A. K. Dhara and S. K. Ghosh, Phys. Rev. A **35**, 442 (1987).
[53]A. Macias and A. Riera, Phys. Rep. **90**, 299 (1982).
[54](a) W. Kohn and P. Vashishta, in Ref. 6, p. 79; (b) A. K. Theophilou, in Ref. 11, p. 201; (c) E. K. U. Gross, L. N. Oliveira, and W. Kohn, Phys. Rev. A **37**, 2805, 2809 (1988); (d) L. W. Oliveira, E. K. U. Gross, and W. Kohn, *ibid.* **37**, 2821 (1988).
[55]D. Tiszauer and K. C. Kulander, Phys. Rev. A **29**, 2909 (1984).
[56]While the computations on the present project were nearing completion, we came across two papers dealing with NLSE's in the context of fluid dynamics. Himi and Fukushima, Nucl. Phys. A **431**, 161 (1984) employ TDHF equations to arrive at the familiar QFD equations governing the time evolution of the density and the velocity field. A point of similarity between their work and ours is the use of the polar form in Eq. (8a) to combine the two QFD equations into a single NLSE. Nonnenmacher and Nonnenmacher, Lett. Nuovo Cimento **37**, 241 (1983) also use the polar form and the Madelung prescription (Ref. 15) to convert the one-dimensional cubic NLSE into two fluid dynamical equations having soliton solutions. The quantum connection, however, is not clear.
[57]The stochastic interpretation of quantum mechanics has a checkered history, somewhat similar to the Madelung interpretation. It was originally suggested by Schrödinger himself and then apparently passed into near oblivion. It was resurrected mainly by I. Fényes, M. Schönberg, and D. Kershaw. Stochastic mechanics received a neat and systematic mathematical structure at the hands of E. Nelson. Subsequent elegant formulation and extension of this viewpoint was carried on by L. de la Peña and others. A considerable body of literature has grown around this viewpoint. For a historical perspective, see M. Jammer, *The Philosophy of Quantum Mechanics,* p. 418 (Wiley, New York, 1974).
[58]There is some controversy about whether the backward diffusion process is truly Markovian or not. Grabert *et al.* [H. Grabert, P. Hanggi, and P. Talkner, Phys. Rev. A **19**, 2440 (1979)] feel that the backward process is not truly Markovian although it has some properties of a Markovian process while Ghirardi *et al.* (see Ref. 32) feel that the backward process is indeed Markovian. Nelson's approach, in particular, its physical content, has been criticized by Mielnik and Tengstrand [Int. J. Theor. Phys. **19**, 239 (1980)], Lavenda and Santamato [Int. J. Theor. Phys. **23**, 585 (1984)], among others.
[59]L. de la Pena and A. M. Cetto, Rev. Mex. Fis. **31**, 551 (1985).
[60]S. K. Ghosh, M. Berkowitz, and R. G. Parr, Proc. Natl. Acad. Sci. USA **81**, 8028 (1984).
[61]S. K. Ghosh and M. Berkowitz, J. Chem. Phys. **83**, 2976 (1985).
[62]R. G. Parr, Int. J. Quant. Chem. **26**, 687 (1984).
[63]L. E. Reichl, *A Modern Course in Statistical Physics* (University of Texas, Austin, TX, 1980), p. 519.
[64]H. Kohl and R. M. Dreizler, Phys. Rev. Lett. **56**, 1991 (1986).
[65]L. Lapidus and G. F. Pinder, *Numerical Solution of Partial Differential Equations in Science and Engineering* (Wiley, New York, 1982), Chaps. 2 and 4.
[66]S. J. Farlow, *Partial Differential Equations for Scientists and Engineers* (Wiley, New York, 1982), Chap. 5.
[67]R. S. Varga, *Matrix Iterative Analysis* (Prentice Hall, New Jersey, 1962), Chap. 8.
[68]M. Delfour, M. Fortin, and G. Payre, J. Comp. Phys. **44**, 277 (1981).
[69]D. Kosloff and R. Kosloff, J. Comp. Phys. **52**, 35 (1983).
[70]E. Clementi and C. R. Roetti, At. Data Nucl. Data Tables **14**, 174 (1974).
[71]R. K. Dodd, J. C. Eilbeck, J. D. Gibbon, and H. C. Morris, *Solitons and Nonlinear Wave Equations* (Academic, London, 1982).
[72]G. L. Lamb, Jr., *Elements of Soliton Theory* (Wiley, New York, 1980).
[73]P. K. Chattaraj, S. Rao Koneru, and B. M. Deb. J. Comp. Phys. **72**, 504 (1987).
[74]T. G. Winter, C. M. Dutta, and N. F. Lane, Phys. Rev. A **31**, 2702 (1985).
[75]A. Hasegawa, *Plasma Instabilities and Nonlinear Effects* (Springer-Verlag, Berlin, 1975).
[76]P. M. Morse and H. Feshbach, *Methods of Theoretical Physics* (McGraw-Hill, New York, 1953), Pt. II, p. 1263.
[77]H. J. Kreuzer, Nuovo Cimento B **45**, 169 (1978).
[78]H. J. Kreuzer, *Nonequilibrium Thermodynamics and Its Statistical Foundations* (Clarendon, Oxford, 1981), Chap. 12.
[79]A. Tachibana, K. Hori, Y. Asai, T. Yamabe, and K. Fukui, J. Mol. Struc. Theochem **123**, 267 (1985).
[80]B. M. Deb and P. K. Chattaraj, Chem. Phys. Lett. **148**, 550 (1988).